References

[1] Jessup M, Brozena S. Heart failure. N Engl J Med 2003;348:2007–18.
[2] Nian M, Lee P, Khaper N, et al. Inflammatory cytokines and postmyocardial infarction remodeling. Circ Res 2004;94:1543–53.
[3] Kocher AA, Schuster MD, Szabolcs MJ, et al. Neovascularization of ischemic myocardium by human bone-marrow-derived angioblasts prevents cardiomyocyte apoptosis, reduces remodeling and improves cardiac function. Nat Med 2001;7:430–6.
[4] Orlic D, Kajstura J, Chimenti S, et al. Mobilized bone marrow cells repair the infarcted heart, improving function and survival. Proc Natl Acad Sci USA 2001;98:10344–9.
[5] Ohtsuka M, Takano H, Zou Y, et al. Cytokine therapy prevents left ventricular remodeling and dysfunction after myocardial infarction through neovascularization. FASEB J 2004;18:851–3.
[6] Minatoguchi S, Takemura G, Chen XH, et al. Acceleration of the healing process and myocardial regeneration may be important as a mechanism of improvement of cardiac function and remodeling by postinfarction granulocyte colony-stimulating factor treatment. Circulation 2004;109:2572–80.
[7] Iwanaga K, Takano H, Ohtsuka M, et al. Effects of G-CSF on cardiac remodeling after acute myocardial infarction in swine. Biochem Biophys Res Commun 2004;325:1353–9.
[8] Harada M, Qin Y, Takano H, et al. G-CSF prevents cardiac remodeling after myocardial infarction by activating the Jak–Stat pathway in cardiomyocytes. Nat Med 2005;11:305–11.
[9] Sugano Y, Anzai T, Yoshikawa T, et al. Granulocyte colony-stimulating factor attenuates early ventricular expansion after experimental myocardial infarction. Cardiovasc Res 2005;65:446–56.
[10] Kawada H, Fujita J, Kinjo K, et al. Nonhematopoietic mesenchymal stem cells can be mobilized and differentiate into cardiomyocytes after myocardial infarction. Blood 2004;104:3581–7.
[11] Kang HJ, Kim HS, Zhang SY, et al. Effects of intracoronary infusion of peripheral blood stem-cells mobilised with granulocyte-colony stimulating factor on left ventricular systolic function and restenosis after coronary stenting in myocardial infarction: the MAGIC cell randomised clinical trial. Lancet 2004;363:751–6.
[12] Hill JM, Syed MA, Arai AE, et al. Outcomes and risks of granulocyte colony-stimulating factor in patients with coronary artery disease. J Am Coll Cardiol 2005;46:1643–8.
[13] Murry CE, Soonpaa MH, Reinecke H, et al. Haematopoietic stem cells do not transdifferentiate into cardiac myocytes in myocardial infarcts. Nature 2004;428:664–8.
[14] Balsam LB, Wagers AJ, Christensen JL, et al. Haematopoietic stem cells adopt mature haematopoietic fates in ischaemic myocardium. Nature 2004;428:668–73.
[15] Frangogiannis NG, Smith CW, Entman ML. The inflammatory response in myocardial infarction. Cardiovasc Res 2002;53:31–47.
[16] Kuroiwa M, Okamura T, Kanaji T, et al. Effects of granulocyte colony-stimulating factor on the hemostatic system in healthy volunteers. Int J Hematol 1996;63:311–6.
[17] Valgimigli M, Rigolin GM, Cittanti C, et al. Use of granulocyte-colony stimulating factor during acute myocardial infarction to enhance bone marrow stem cell mobilization in humans: clinical and angiographic safety profile. Eur Heart J 2005;26:1838–45.
[18] Kuethe F, Figulla HR, Herzau M, et al. Treatment with granulocyte colony-stimulating factor for mobilization of bone marrow cells in patients with acute myocardial infarction. Am Heart J 2005;150(115): e1–e7.
[19] Ince H, Petzsch M, Kleine HD, et al. Preservation from left ventricular remodeling by front-integrated revascularization and stem cell liberation in evolving acute myocardial infarction by use of granulocyte-colony-stimulating factor (FIRSTLINE-AMI). Circulation 2005;112:3097–106.
[20] Zohlnhofer D, Ott I, Mehilli J, et al. Stem cell mobilization by granulocyte colony-stimulating factor in patients with acute myocardial infarction: a randomized controlled trial. JAMA 2006;295:1003–10.
[21] Ripa RS, Jorgensen E, Wang Y, et al. Stem cell mobilization induced by subcutaneous granulocyte-colony stimulating factor to improve cardiac regeneration after acute ST-elevation myocardial infarction. Result of the double-blind, randomized, placebo-controlled stem cells in myocardial infarction (STEMMI) trial. Circulation 2006;113:1983–92.
[22] Wenaweser P, Rey C, Eberli FR, et al. Stent thrombosis following bare-metal stent implantation: success of emergency percutaneous coronary intervention and predictors of adverse outcome. Eur Heart J 2005;26:1180–7.

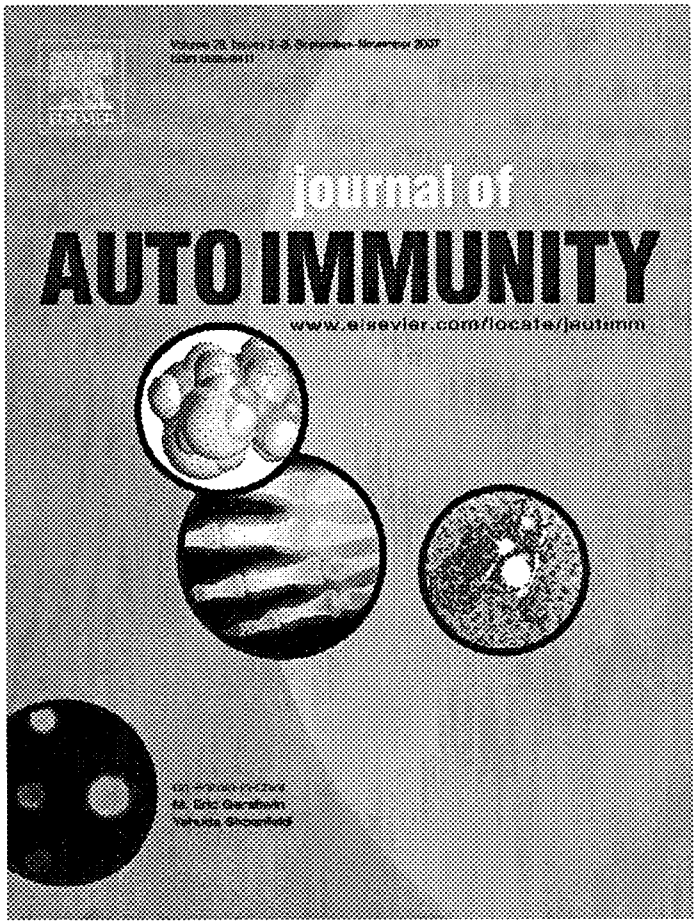

ELSEVIER

Journal of Autoimmunity 29 (2007) 146–153

journal of autoimmunity

www.elsevier.com/locate/jautimm

Th1-type immune responses by Toll-like receptor 4 signaling are required for the development of myocarditis in mice with BCG-induced myocarditis

Kimiaki Nishikubo [a], Kyoko Imanaka-Yoshida [b], Shigenori Tamaki [a], Michiaki Hiroe [c], Toshimichi Yoshida [b], Yukihiko Adachi [d], Yasuhiro Yasutomi [e,f,*]

[a] *Department of Rheumatology, National Hospital Organization, Mie Chuo Medical Center, Mie 514-1101, Japan*
[b] *Department of Pathology, Mie University Graduate School of Medicine, Mie 514-8507, Japan*
[c] *Department of Nephrology and Cardiology, International Medical Center of Japan, Tokyo 162-8655, Japan*
[d] *Department of Gastroenterology and Hepatology, Mie University Graduate School of Medicine, Mie 514-8507, Japan*
[e] *Department of Bioregulation, Mie University Graduate School of Medicine, Mie 514-8507, Japan*
[f] *Laboratory of Immunoregulation and Vaccine Research, Tsukuba Primate Research Center, National Institute of Biomedical Innovation, Tsukuba, Ibaraki 305-0843, Japan*

Received 31 March 2007; revised 1 July 2007; accepted 1 July 2007

Abstract

The immunological aspects of autoimmune myocarditis are difficult to understand because of the existence of many infectious agents and animal models suggesting different mechanisms in autoimmune myocarditis. To overcome these difficulties, two strains of mice, C3H/HeN and C3H/HeJ, showing different immune responses to mycobacteria, were immunized with myosin mixed with BCG. The C3H/HeN mice with a wild-type Toll-like receptor 4 (TLR4) showed severe myocarditis, whereas the C3H/HeJ mice with nonfunctional mutated TLR4 did not. $CD4^+$ cells from both strains of mice exhibited appreciable proliferative responses following myosin stimulation; however, the cytokines from these cells differed between these two strains. The C3H/HeN mice showed T helper (Th)1-type cytokine responses, whereas the expressions of mRNA in C3H/HeJ mice were Th2-type cytokine. When both of these strains of immunized mice were inoculated with a plasmid encoding cDNA of interleukin (IL)-4 or agonistic IL-4, the development of myocarditis was inhibited in C3H/HeN mice. Moreover, C3H/HeJ mice, in which development of myocarditis was not induced by immunization of myosin mixed with BCG, showed myocarditis after injection of IL-4 antagonistic mutant DNA for the induction of Th1-type immune responses. The results suggested that the induction of autoimmune myocarditis by myosin is affected by Th1-type immune responses.

Keywords: Autoimmunity; Bacillus Calmette–Guérin; Myocarditis; Th1/Th2; TLR4

1. Introduction

Myocarditis is a potentially lethal disorder of various etiologies for which no treatment is currently satisfactory [1]. Although the etiology of dilated cardiomyopathy is unknown, more than 10% of cases are associated with a previous virus infection, such as Coxsackievirus B3 [2]. Since heart failure generally occurs long after infection with autoimmune responses, autoimmunity is thought to play an important role in myocarditis as well as contributing to the progression to cardiomyopathy and heart failure [3]. To explore the mechanisms

Abbreviations: DC, dendritic cell; DTH, delayed-type hypersensitivity; EAM, experimental autoimmune myocarditis; TLR, Toll-like receptor.

* Corresponding author. Laboratory of Immunoregulation and Vaccine Research, Tsukuba Primate Research Center, National Institute of Biomedical Innovation, 1-1 Hachimandai, Tsukuba, Ibaraki 305-0843, Japan. Tel.: +81 29 837 2121; fax: +81 29 837 0218.

E-mail addresses: yasutomi@doc.medic.mie-u.ac.jp, yasutomi@nibio.go.jp (Y. Yasutomi).

0896-8411/$ - see front matter © 2007 Elsevier Ltd. All rights reserved.
doi:10.1016/j.jaut.2007.07.001

of such immune system-mediated damage to the heart in this disease, various animal models have been established by infection of various pathogens and immunization of cardiac myosin (reviewed in [4]). Although animal models of experimental autoimmune myocarditis (EAM) have provided information on pathogenesis that is valuable for the prevention and treatment of myocarditis, an understanding of the pathogenesis of EAM in animal models is difficult to apply to human myocarditis. Animal models of EAM have been established in various species and strains of animals using various types of infectious pathogens and immunization of cardiac myosin, and the pathogenic mechanisms in these models have not shown identical immune responses [5,6]. To overcome these difficulties, animal models of EAM that are established for understanding immune response to myocytes should allow us to identify several factors that induce EAM such as pathogens and the genetic basis of animals.

T helper (Th) cells are thought to have crucial roles in both autoimmune diseases and immunological disorders. Th cells are identified by functions as Th1 or Th2 subsets secreting distinct cytokine patterns that demonstrate effector functions and cross inhibition [7]. Cytokines are important for controlling the response of Th cells to self antigens (Ags) and they play a critical role in shifting the immune response toward a Th1 or Th2 pattern. A Th1 response shifts the cytokine profile toward delayed-type hypersensitivity (DTH), macrophage activation, and proinflammatory T-cell response associated with interferon (IFN)-γ and interleukin (IL)-2 and -12, whereas a Th2 response is associated with B cell activation and humoral immunity and with IL-4, -5, -9, -13 and IgE production. As a result, understanding the Th cell responses to auto-Ags is important for the prevention and treatment of autoimmune diseases such as autoimmune myocarditis in human patients.

Mice with a C3H/He lineage were originally established in 1941, and two laboratories have maintained this strain as C3H/HeN and C3H/HeJ since 1947 and 1951, respectively. These two strains of mice showed different responses to some strains of bacteria, and the differences in the responses to some strains of bacteria have been thought to be caused by Toll-like receptor (TLR) 4 [8]. C3H/HeJ mice have an unfunctional TLR4 [9], and these mice are more susceptible to mycobacteria infection than are TLR4 wild-type mice [10–12]. TLR activation elicits adaptive immune responses with a bias towards Th1 T-cell response. It has also been reported that TLR4 wild-type C3H/HeN mice, but not mutated TLR4 C3H/HeJ mice, showed typical Th1-type immune responses to mycobacteria infection [10,12,13], although both strains of mice have the wild-type Bacillus Calmette–Guérin (BCG) resistant gene *(N-ramp)*.

To elucidate the immunological mechanisms by which cardiac myosin is recognized without various factors, we tried to establish an animal model of EAM by using the responses to mycobacteria in the present study. Two strains of mice, mycobacteria-susceptible C3H/HeJ mice and mycobacteria-resistant C3H/HeN mice, were immunized with porcine cardiac myosin mixed with BCG. Interestingly, mycobacteria-resistant C3H/HeN mice, but not mycobacteria-susceptible C3H/HeJ mice, developed myocarditis. We herein report the differences in immune responses to myosin in the development of an animal model of EAM in mice with a close genetic background.

2. Materials and methods

2.1. Mice

Six- to eight-week-old C3H/HeN (TLR4 wild type) and C3H/HeJ (TLR4 mutated) female mice were purchased from CLEA Japan (Osaka, Japan) and housed in the Laboratory Animal Center of Mie University School of Medicine.

2.2. Immunization of myosin

Each mouse was immunized with 100 μg of porcine cardiac myosin (Sigma) mixed with 1 mg of BCG Tokyo strain (Japan BCG Laboratory, Tokyo, Japan) in IFA into the footpad on day 0 and day 14. The BCG used for immunization was well-ground and killed. This myosin and BCG mixture was completely emulsified with IFA. The injection site (footpad) and degree of emulsification are very important for the development EAM. The control mice were injected with the same amount of BCG alone in emulsified IFA. All mice were sacrificed on day 21 for pathological observations (Fig. 1a).

2.3. Administration of DNA

The plasmids encoding cDNA of antagonistic interleukin (IL)-4 double mutant (Q116D/Y119D) (IL-4DM) and agonistic IL-4 single mutant (Q116D) (IL-4SM) have been described previously [14]. The mice were intraperitoneally administered 100 μg of plasmid DNA encoding IL-4, IL-4SM or IL-4 DM on days −7, 0, 7 and 14 to regulate the Th balances. An empty plasmid (pcDNA 3.1) vector was used as a control (Fig. 1b).

2.4. Proliferative responses of spleen cells to porcine myosin

The responding spleen cells obtained from the immunized mice were depleted of $CD4^+$ or $CD8^+$ cells using a commercially available system of magnetic bead-coupled specific antibodies (Abs) to confirm the subset of effector cells. The purity of cells (CD4 or CD8 cells) was confirmed by FACS analysis. The proportion of targeted cells did not exceed 0.01%, and dead cells were removed after cell washing (viability >90%). The cells were resuspended in complete medium and cultured at a concentration of 2×10^5 cells per culture well in a total volume of 0.2 ml with 10 μg/ml of myosin. The same amount of OVA was used as a control Ag. Each culture was performed in triplicate in 96-well microculture plates and was then maintained in a humidified atmosphere of 5% CO_2 at 37 °C. The cultures were harvested using a cell harvester at 96 h after a 6-h pulse with 18.5 kBq/well of [^{3}H]thymidine. The results were calculated from the uptake of [^{3}H]thymidine and expressed as the mean uptake in cpm ± SD of triplicate cultures.

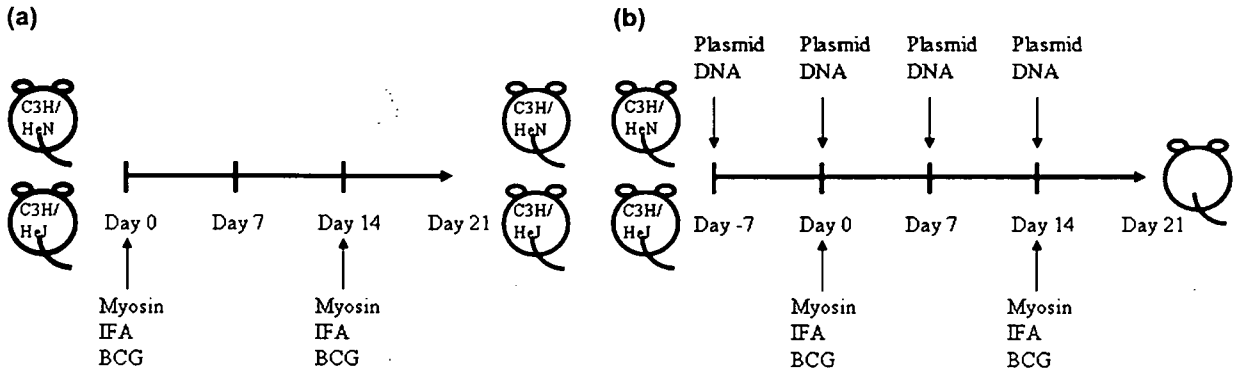

Fig. 1. Experimental design in this study. (a) Each mouse was immunized with 100 μg of porcine cardiac myosin mixed with 1 mg of BCG in IFA into the footpad on day 0 and day 14 (see Section 2). (b) Plasmid DNA of IL-4, IL-4SM, IL-4DM or control was intraperitoneally injected once on days −7, 0, 7 and 14.

2.5. Detection of cytokine mRNA from lymphocytes using RT–PCR

Total RNA was purified from the OVA (control)- or myosin-stimulated spleen cells using Isogen (Nippongene, Japan) following the manufacturer's instructions. For the RT reaction, a reverse transcription system (Promega, WI, USA) was used. PCR was performed in a total volume of 50 μl of 1× PCR buffer (Takara Shuzo, Japan) containing 0.5–1.0 μg of cDNA, 0.25 mM of each dNTP, 2 μM of each primer, and 2.5 U of *Taq* DNA polymerase (Takara Shuzo, Japan). The specific primer pairs used were as follows: IL-2, 5′-AAGAT GAACTTGGACCTCTGCGG-3′ (sense) and 5′-CCTTATG TGTTGTAAGCAGGAGG-3′ (antisense); IL-4, 5′-ATGGGT CTCAACCCCCAGCTAGT-3′ (sense) and 5′-GCTCTTTAG GCTTTCCAGGAAGTC-3′ (antisense); IL-12p40, 5′-TCC TGCACTGCTGAAGACATC-3′ (sense) and 5′-TCTCGCCA TTATAGATTCAGAGAC-3′ (antisense); IL-13, 5′-GACCCA GAGGATATTGCATG-3′ (sense) and 5′-CCAGCAAAGTCT GATGTGAG-3′ (antisense); and mouse HPRT, 5′-GATAC AGGCCAGACTTTGTTGG-3′ (sense) and 5′-GAGGGTA GGCTGGCCTATAGG-3′ (antisense). The samples were amplified for 30–35 cycles under the following conditions: annealing for 30 s at 56 °C, extension for 1 min at 73 °C, and denaturation for 30 s at 93 °C. The reaction products were analyzed on 2% agarose, Tris-buffered EDTA TBE gel.

2.6. Measurement of interferon-γ (IFN-γ)

Spleen cells from immunized mice (5×10^6) were cultured with 10 μg/ml of myosin in 24-well culture plates at a volume of 2 ml. After incubation at 37 °C in a humidified incubator (5% CO_2) for 96 h, culture supernatants were quantified by using a standard ELISA kit (BioSource International, CA, USA).

2.7. Statistical analysis

Statistical analysis was performed using the Mann–Whitney *U*-test and the Kruskal–Wallis test. The values are expressed as means ± SD. A 95% confidence limit was considered to be significant ($p < 0.05$).

3. Results

3.1. Development of EAM

Although rodent models of EAM have been established in various species and strains, it is not easy to understand the mechanisms underlying the development of EAM by recognition of autologous myosin Ags because of the effects of genetic backgrounds. To determine whether cardiac myosin immunization can induce EAM in strains of mice with the same genetic background except for TLR4, C3H/HeN and C3H/HeJ mice were immunized with cardiac myosin mixed with BCG. The histological findings were classified into severe (>50%), moderate (10–49%) and mild (<9%) depending on the ratio of affected area to total myocardium. The C3H/HeN mice developed mild (2/20), moderate (14/20) and severe (4/20) myocarditis, whereas only one C3H/HeJ mouse showed mild myocarditis (1/20) by histopathological observations on day 21 (Fig. 2). Two C3H/HeN mice died before sacrifice on day 18 (severe and moderate myocarditis). Moreover, EAM did not develop in either strain of mice immunized with myosin and IFA without BCG, and the control mice immunized with IFA emulsion containing BCG or myosin alone did not show any abnormalities (data not shown). These results demonstrated that immunization of an emulsion containing myosin and BCG induced the development of EAM in wild-type C3H/HeN mice but not in TLR4-mutated C3H/HeJ mice.

3.2. Myosin-specific spleen cell proliferative responses in myosin-immunized mice

We next confirmed the presence of effector cells that recognize the myosin induced by the immunization of myosin mixed with BCG in *in vivo* experiments. Spleen cells from both strains of mice immunized with myosin mixed with BCG were assessed for their proliferative responses after stimulation *in vitro* with myosin. Spleen cells from both C3H/HeN mice with myocarditis and C3H/HeJ mice without myocarditis exhibited proliferative responses after *in vitro* stimulation with myosin (Fig. 3). These proliferative responses were not observed in the case of stimulation with an irrelevant Ag

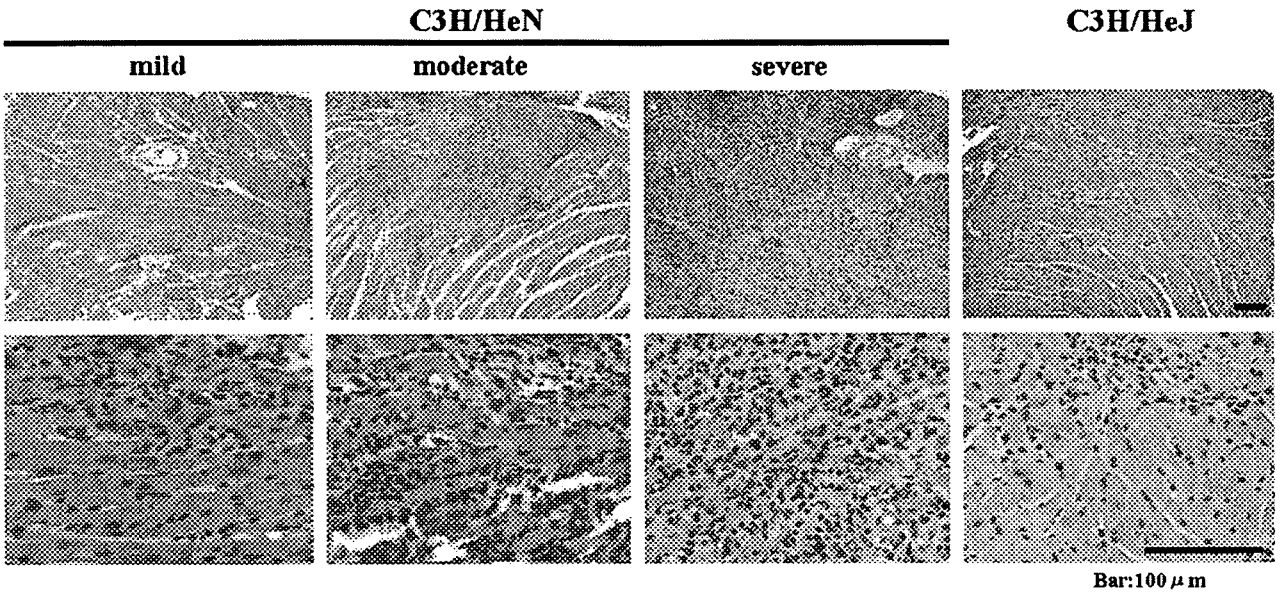

Fig. 2. Results of histopathological examination of hearts from mice that had been immunized with cardiac myosin mixed with BCG in IFA. The histological findings were classified into severe (>50%), moderate (10–49%) and mild (<9%) depending on the ratio of affected area to total myocardium. All tissue specimens were obtained 21 days after the first myosin immunization. The tissue specimens were fixed in 10% formalin, embedded in paraffin, sectioned, and stained with hematoxylin and eosin. These results are representative of five independent experiments. Bars represent 100 μm.

(OVA). A significant component of this proliferative response was attributed to the presence of $CD4^+$ cells, because $CD4^+$ cell-depleted spleen cells exhibited a substantially reduced myosin-specific proliferative response. Moreover, the C3H/HeN mice did not develop myocarditis when they received a monoclonal Ab to CD4 for depleting $CD4^+$ cells (data not shown). The observation that immunization of myosin mixed with BCG in both strains of mice elicited a $CD4^+$ proliferative T-lymphocyte response suggested that myosin mixed with BCG induces a myosin-specific Th cell response in not only mice with myocarditis but also in mice without myocarditis.

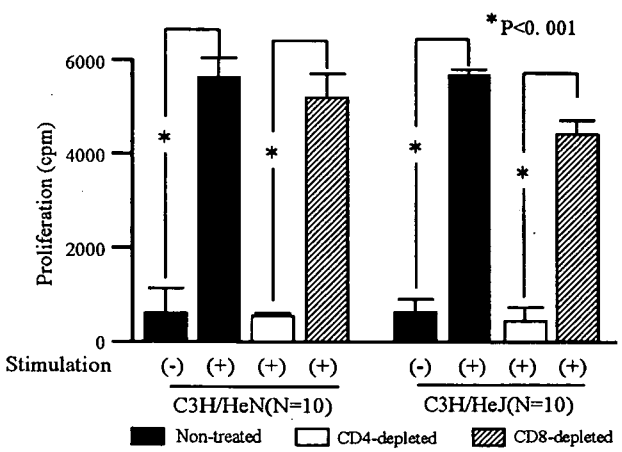

Fig. 3. Myosin-immunized mice develop $CD4^+$, myosin-specific spleen cell proliferative responses. Responding spleen cells were depleted of $CD4^+$ or $CD8^+$ cells using a commercially available system of magnetic bead-coupled specific Abs and co-cultured with myosin. Each value is the mean cpm ± SE of ten mice/group. $*p < 0.001$.

3.3. Myosin-specific cytokine responses of spleen cells from immunized mice

To elucidate the immunological qualities of myosin-specific $CD4^+$ T cells, myosin-specific cytokine responses were analyzed in experimental mice. The responses of myosin-specific cytokines in spleen cells obtained from the experimental mice on day 21 were examined by two different methods. The production of IFN-γ from spleen cells after stimulation *in vitro* with myosin or OVA (control) was assessed by ELISA. Spleen cells from C3H/HeN mice with myocarditis immunized with myosin mixed with BCG produced a significantly larger amount of IFN-γ in the supernatant of the culture than did spleen cells from C3H/HeJ mice without myocarditis after stimulation *in vitro* with myosin (Fig. 4a). We next assessed the mRNA expression levels of Th1-type cytokines (IL-2 and -12) and Th2-type cytokines (IL-4 and -13) in spleen cells after *in vitro* stimulation with myosin or OVA (control). Spleen cells from C3H/HeN mice with myocarditis showed strong IL-2 and -12 expression and weak IL-4 and -13 expression of mRNA, whereas completely opposite results were obtained for spleen cells from C3H/HeJ mice without myocarditis. Spleen cells from C3H/HeJ mice without myocarditis showed strong expression of mRNA of Th2-type cytokines (IL-4 and -13) and weak expression of Th1-type cytokines (IL-2 and -12). Moreover, spleen cells from C3H/HeN mice treated with myosin and IFA without BCG showed Th2-type immune responses (data not shown). Upstream of the release of some Th1-type cytokines are the TLRs, and C3H/HeN mice with wild-type TLR4 developed EAM while also showing a Th1-type immune response to myosin. Although induction of another T-cell linage, Treg, was also assessed by the expression

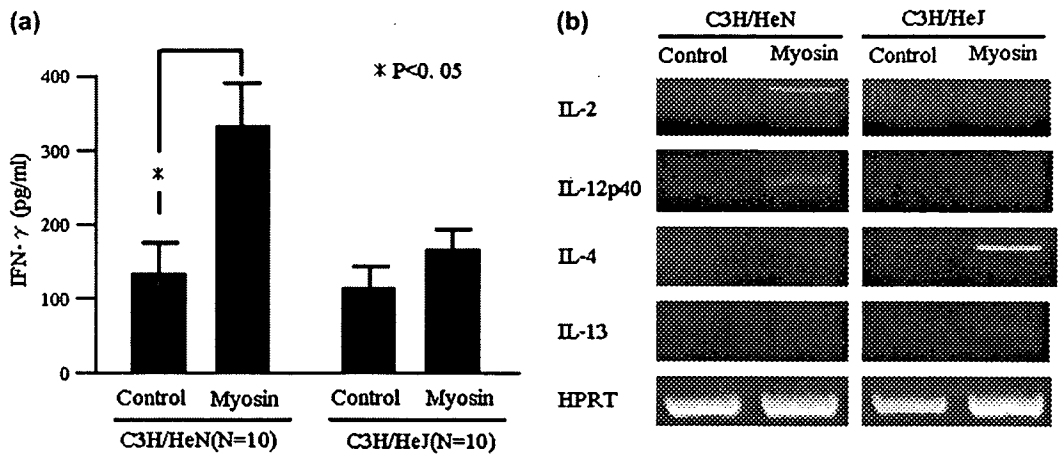

Fig. 4. Cytokine production in culture supernatant and expression of mRNAs of cytokines from spleen cells. (a) The amount of IFN-γ in the culture supernatant was measured by ELISA 21 days after the first myosin immunization. Each value shown is the mean and SD of ten mice per group. (b) Spleen cells were stimulated *in vitro* with myosin for 1 day in culture. Spleen cells stimulated with OVA were used as controls. The reaction products were analyzed on 2% agarose, Tris-buffered EDTA TBE gels. The profiles are representative of three independent experiments.

of mRNA of IL-10 and transforming growth factor-β, these cytokines were not different in C3H/HeN mice with myocarditis and C3H/HeJ mice without myocarditis (data not shown). These results indicated that the $CD4^+$ cells of C3H/HeN mice (TLR4 wild type) and C3H/HeJ mice (TLR4 unfunctional mutated) were polarized toward different Th responses after immunization by an emulsion of myosin mixed with BCG followed by proliferation.

3.4. Effects of IL-4, IL-4SM or IL-4DM DNA administration on the development of myocarditis in mice immunized with myosin mixed with BCG

To examine the effects of regulating Th responses using IL-4, IL-4SM (agonistic IL-4 single mutant) and IL-4DM (antagonistic IL-4 double mutant) DNA on the development of myocarditis in both strains of mice immunized with myosin mixed with BCG, the mice were intraperitoneally administered 100 μg of DNA vaccine or control plasmid on days −7, 0, 7 and 14 (Fig. 1b). The IL-4 mutant Q116D/Y119D, which forms unproductive complexes with the IL-4Rα-chain, acts as an antagonist by inhibiting the formation of heterodimers with other receptors [15]. These IL-4-binding inhibitors act not only by inhibiting IL-4 binding to its receptor but also by preventing IL-13 from eliciting its activity, since the IL-4Rα-chain also forms a functional signaling component of the IL-13R heterodimer [16,17]. We previously reported that such plasmid administration can regulate the systemic Th immune responses in autoimmune and allergic diseases by only a single injection [14]. C3H/HeN mice, in which the development of myocarditis was induced by immunization of myosin mixed with BCG, did not develop myocarditis when they were injected with the IL-4 and IL-4SM (agonistic IL-4 mutant) DNA vaccines to inhibit the Th1-type immune response ($n = 10$ respectively) (Fig. 5). On the other hand, C3H/HeJ mice, in which the development of myocarditis was not induced by the same immunization, were not affected by the injection of IL-4 and IL-4SM DNA vaccines ($n = 10$ respectively). However, surprisingly, C3H/HeJ mice developed myocarditis (mild in 3/10 and moderate in 7/10) when they were injected with antagonistic IL4 mutant, IL-4DM, DNA vaccine for inhibition of Th2-type immune responses by prevention of IL-4 signaling (Fig. 5). The injection of control plasmid did not influence the development of myocarditis in either strain of mice ($n = 10$ respectively) (Fig. 5). Mice did not develop myocarditis without BCG in any plasmid DNA injected (data not shown). These results were derived by four injections of DNA, although the experimental model of allergic inflammation was inhibited by only a single injection of DNA. We previously reported that administration of IL-4DM DNA did not change the Ag-specific Th responses in cytokine production by *in vitro* stimulation of Ag without the presence of IL-4DM protein [14]. In fact, the results for myosin-specific cytokine production from spleen cells of both strains of mice administered IL-4, IL-4SM or IL-4DM DNA vaccines were the same as the results shown in Fig. 4 (without injection of DNA vaccines) after *in vitro* stimulation of myosin (data not shown). The existence of a small amount of IL-4 or IL-4 mutant for a long time *in vivo* might have played a role in the development of EAM. Since pharmacokinetic half-lives of IL-4 and IL-4 mutant proteins are very short *in vivo* ($t_{1/2} = 0.83$ h), a high concentration of these molecules in plasma must be maintained for a long period in order for effects on various phenotypes to be obtained. These effects usually disappeared immediately after discontinuing administration of these proteins. The antagonistic IL-4 is more effective than neutralizing Ab to IL-4, and commercially available Abs to IL-4 do not have sufficient effects to inhibit the activity of IL-4. These results indicated that the regulation of functions of IL-4 played an important role in the development of myocarditis induced by the immunization of myosin mixed with BCG in the strains of C3H/He mice. These results also indicated the possibility

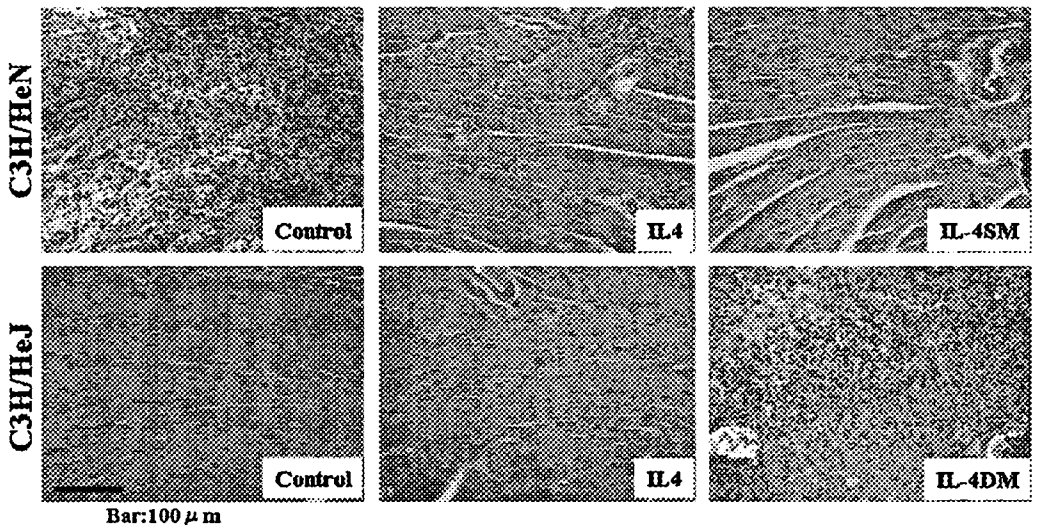

Fig. 5. Results of histopathological examination of hearts from myosin-immunized mice that had been administered IL-4, IL-4SM, IL-4DM or control. All tissue specimens were obtained 21 days after the first myosin immunization. The tissues specimens were fixed in 10% formalin, embedded in paraffin, sectioned, and stained with hematoxylin and eosin. Mice that had been immunized with myosin mixed with BCG in IFA were each injected with 100 μg of IL-4, IL-4SM, IL-4DM or control plasmid DNA four times on days −7, 0, 7 and 14. These results are representative of three independent experiments. Bars represent 100 μm.

that myocarditis is associated with Th1-type $CD4^+$T-cells in these strains of mice.

4. Discussion

$CD4^+$ T cells have been reported to be required for the induction of EAM in mice. The development of EAM in A/J mice was prevented by the depletion of $CD4^+$ T cells, and disease severity was reduced by depleting $CD8^+$T cells (reviewed in [18,19]). A widely held belief is that when the cytokine profile of autoreactive T cells shifts toward an inflammatory Th1 type, the result is pathogenicity and autoimmune diseases (reviewed in [20,21]). Autoimmune myocarditis in the Lewis rat model was promoted by Th1-type immune responses in the same manner as that seen in our experiments [22]. On the other hand, it is difficult to understand the development of myocarditis in the EAM mouse model based on the Th1/Th2 paradigm. Although Th2-type immune responses played a critical role in the development of myocarditis in the mouse model of EAM using A/J and BALB/C strains [23,24], Th1-type immune responses were also suggested to participate in the development of EAM. Moreover, it has been reported that another novel population of T cells, regulatory T cell (Treg), are also important for controlling development of EAM as well as other disease [25–30]. These reports suggested that loss of immune tolerance regulated by Treg cells are one of the mechanisms of development of EAM. It has been reported that EAM did not develop in mice deficient in the Th1-type cytokine IL-12 or its receptor after administration of myosin or myosin Ag peptide, and that the CC-chemokine secreted by Th1-type T cells mediates EAM [31–33]. These differences in immune responses in EAM models are thought to be due to the correlation between mouse strain and mycobacteria species. The EAM model of A/J was established by using a large amount of virulent mycobacteria (*Mycobacterium tuberculosis*), and a small amount of the same bacteria was used for BALB/c mice. We used avirulent *Mycobacteria bovis* BCG (vaccine strain) for establishment of EAM. The A/J mouse strain is susceptible to *Mycobacterium tuberculosis* and resistant to BCG. C3H/HeN mice are resistant to both strains of mycobacteria with the same responses as those in humans, and BALB/c mice show responses opposite to those of A/J mice (resistant to *Mycobacterium tuberculosis* and susceptible to BCG) [34–36]. These differences are dependent on various genetic factors such as *Nramp* gene.

Some studies have suggested a relationship between TLR4 and myocarditis. Infection with a Coxsackievirus, which is a well-known agent of myocarditis, was found to upregulate TLR4 on mast cells and macrophages immediately following infection. TLR4 signaling also increases the occurrence of acute myocarditis and production of proinflammatory cytokines in the heart [37]. Moreover, the critical requirement of TLR4 signaling in dendritic cells (DCs) for myocarditis induction was genetically proven by the fact that myosin Ag peptide (MYHC-α)-pulsed and TLR4/CD40-activated DCs isolated from TLR4-deficient mice did not induce myocarditis in wild-type recipients when DCs isolated by the same procedure from TLR4-wild type transfer elicited myocarditis in a wild-type recipient [38]. In our system, two important points regarding the establishment of EAM were observed. Porcine myosin must be mixed well in IFA, and EAM was only observed by immunization of this emulsion into the footpad. These observations suggest that myosin Ag is incorporated in the same APCs such as macrophages or DCs together with BCG for a long period of time as oil particles, and then myosin-specific immune responses are induced by the influence of the characteristic immune responses of a large quantity of BCG associated with TLR4.

Relationships between TLRs and mycobacteria have been reported. TLR2, TLR4 and TLR1/TLR6 heterodimers with

TLR2 have been implicated in the recognition of mycobacterial Ags [39]. The emerging concept of TLRs as key molecules for shaping the quality of immune responses against microbes is further supported by results of experiments showing that mice lacking MyD88 are incapable of developing Ag-specific Th1 responses after immunization with OVA mixed with CFA (containing dead mycobacteria as an active component) [40]. These results are thought to be due to a mechanism involving both TLR2 and TLR4, since CFA contains a complex mixture of mycobacterial components, some of which are recognized by different members of the Toll family, TLR2 and TLR4. The EAM established in our system utilized these TLRs by immunization with extremely large amounts of BCG and cardiac myosin as a mixed emulsion, thus suggesting the importance of TLR4 for the induction of Th1-type immune responses related to EAM. The C3H/HeJ mouse, which has unfunctional TLR4, showed Th2-type immune responses to myosin after immunization of cardiac myosin mixed with BCG (Fig. 4). Mycobacteria induce Th1-type immune responses through TLR2 and TLR4 stimulation; however, our results showed Th2-type immune responses through TLR2 stimulation without TLR4 by BCG as an adjuvant. Similar results have also been reported by other investigators. Th2-type cytokines were induced from DCs by mycobacteria dependent on TLR2-mediated recognition but not TLR4-mediated recognition [41]. In our experiment, TLR4 mutant C3H/HeJ and wild-type C3H/HeN mice were used for analysis of Th responses in EAM. Unfunctional TLR4 mutations in humans have also been reported (reviewed in [42]). Studies using TLR4 knockout mice are needed to clarify this. Since the commonly used mouse background to generate knockout mice is associated with an increased susceptibility to mycobacteria, extensive backcrossing of such mice is required [43].

Many animal models of myocarditis are available to investigate the optimal therapy for myocarditis. However, the establishment of new animal models of myocarditis is still necessary to better understand myocarditis, because the understanding of myocarditis in humans is still insufficient. In the present study, we utilized two strains of C3H/He mice, which showed different susceptibilities to BCG, for the establishment of EAM involving Th1-type immune responses. The results of this study provide evidence of the potential utility of studying immunological mechanisms in order to both treat and prevent myocarditis.

Acknowledgments

This work was supported by Health Science Research Grants from the Ministry of Health, Labor and Welfare of Japan and the Ministry of Education, Culture, Sports, Science and Technology of Japan.

References

[1] Brown CA, O'Connell JB. Myocarditis and idiopathic dilated cardiomyopathy. Am J Med 1995;99:30–314.
[2] Felker GM, Hu W, Hare JM, Hruban RH, Baughman KL, Kasper EK. The spectrum dilated cardiomyopathy. The Johns Hopkins experience with 1278 patients. Medicine 1999;78:270–83.
[3] Caforio AL, Goldman JH, Haven AJ, Baig KM, Libera LD, McKenna WJ. Circulating cardiac-specific autoantibodies as markers of autoimmunity in clinical and biopsy-proven myocarditis. The Myocarditis Treatment Trial Investigators. Eur Heart J 1997;18:270–5.
[4] Rose NL, Susan LH. Autoimmune myocarditis. Int J Cardiol 1996;54: 171–5.
[5] Pontes-De-Carvalho L, Santana CC, Soares MBP, Oliveria GGS, Cunha-Neto C, Ribeiro-Dos-Santos R. Experimental chronic Chagas' disease myocarditis is an autoimmune disease preventable by induction of immunological tolerance to myocardial antigen. J Autoimmun 2002;18:131–8.
[6] Fairweather D, Kaya Z, Shellam GR, Lawson CM, Rose NR. From infection to autoimmunity. J Autoimmun 2001;16:175–86.
[7] Skaguchi S. Regulatory T cells: key controllers of immunologic self tolerance. Cell 2000;101:125–31.
[8] Janssens J, Beyaert R. Role of Toll-like receptors in pathogen recognition. Clin Microbiol Rev 2003;16:637–46.
[9] Poltrak A, He X, Smirnova I, Liu MY, Huffel CV, Du X, et al. Defective LPS signaling in C3H/HeJ and C57BL/10ScCr mice: mutation in Tlr4 gene. Science 1998;282:2085–8.
[10] Abel B, Thieblemont N, Quesniaux VJF, Brown N, Mpagi J, Miyake K, et al. Toll-like receptor 4 expression is required to control chronic *Mycobacterium tuberculosis* infection in mice. J Immunol 2002;169:3155–62.
[11] Fremond MCC, Nicole DMM, Torres DS, Quesniaux VFJ. Control of *Mycobacterium bovis* BCG infection with increased inflammation in TLR4-deficient mice. Microbes Infect 2003;5:1070–81.
[12] Branger J, Leemans JC, Florquin S, Weijer S, Speelman P, van der Poll T. Toll-like receptor 4 plays a protective role in pulmonary tuberculosis in mice. Int Immunol 2004;16:509–16.
[13] Reiling N, Holscher C, Fehrenbach A, Kroger S, Kirschbibg CJ, Goyert S, et al. Toll-like receptor (TLR)2- and TLR4-mediated pathogen recognition in resistance to airborne infection with *Mycobacterium tuberculosis*. J Immunol 2002;169:3480–4.
[14] Nishikubo K, Murata Y, Tamaki S, Sugama K, Imanaka-Yoshida K, Yuda N, et al. A single administration of interleukin-4 antagonistic mutant DNA inhibits allergic airway inflammation in a mouse model of asthma. Gene Ther 2003;10:2119–25.
[15] Grunewald SM, Kunzmann S, Schnarr B, Ezernieks J, Sebald W, Duschl A. A murine interleukin-4 antagonistic mutant protein completely inhibits interleukin-4 induced cell proliferation, differentiation, and signal transduction. J Biol Chem 1997;272:1480–3.
[16] Nelms K, Keegan AD, Zamorano J, Ryan JJ, Paul WE. The IL-4 receptor: signaling mechanisms and biologic functions. Annu Rev Immunol 1999;17:701–38.
[17] Reiner P, Sebald W, Duschl A. The interleukin-4-receptor: from recognition mechanism to pharmacological target structure. Angew Chem Int Ed 2000;39:2834–46.
[18] Afanasyeva M, Georgakopoulos D, Rose NR. Autoimmune myocarditis: cellular mediators of cardiac dysfunction. Autoimmun Rev 2004;3. 746–486.
[19] Smith SC, Allen PM. Myosin-induced acute myocarditis is a T cell-mediated disease. J Immunol 1991;147:2141–7.
[20] Libleau RS, Singer SM, McDevitt HO. Th1 and Th2 CD4+T cells in the pathogenesis of organ-specific autoimmune diseases. Immunol Today 1995;16:34–8.
[21] Tian J, Olcott AP, Hansenn LR, Zekzer D, Middleton B, Kaufman DL. Infectious Th1 and Th2 autoimmunity in diabetes-prone mice. Immunol Rev 1998;164:119–27.
[22] Liu W, Li WM, Gao C, Sun NL. Effects of atorvastatin on the Th1/Th2 polarization of ongoing experimental autoimmune myocarditis in Lewis rats. J Autoimmun 2005;25:258–63.
[23] Afanasyeva M, Wang Y, Kaya Z, Park S, Zilliox MJ, Schofield BH, et al. Experimental autoimmune myocarditis in A/J mice is an interleukin-4-dependent disease with a Th2 phenotype. Am J Pathol 2001;159:193–203.
[24] Cunningham MW. Cardiac myosin and the TH1/TH2 paradigm in autoimmune myocarditis. Am J Pathol 2001;159:5–12.

[25] Ono M, Shimizu J, Miyachi Y, Sakaguchi S. Control of autoimmune myocarditis and multiorgan inflammation by glucocorticoid-induced TNF receptor family -related protein (high), Foxp3-expressing $CD25^+$ and CD25− regulatory T cells. J Immunol 2006;176:4748–56.
[26] Abbas AK, Lohr J, Knoechel B. Balancing autoaggressive and protective T cell responses. J Autoimmun 2007;28:59–61.
[27] Alvarado-Sanchez B, Hernandez-Castro B, Portales-Perez D, Baranda L, Layseca-Espinosa E, Abud-Mendoza C, et al. Regulatory T cells in patients with systemic lupus erythematosus. J Autoimmun 2006;27:110–8.
[28] Ansari AA, Pereira LE, Mayne AE, Onlamoon N, Pattanapanyasat K, Mori K, et al. The role of disease stage, plasma viral load and regulatory T cells (Tregs) on autoantibody production in SIV-infected non-human primates. J Autoimmun 2007;28:152–9.
[29] Ban Y, Tozaki T, Tobe T, Ban Y, Jacobson EM, Concepcion ES, et al. The regulatory T cell gene FOXP3 and genetic susceptibility to thyroid autoimmunity: An association analysis in Caucasian and Japanese cohorts. J Autoimmun 2007;28:201–7.
[30] Youinou P. B cell conducts the lymphocyte orchestra. J Autoimmun 2007;28:143–51.
[31] Eriksson U, Kurrer MO, Sebald W, Brombacher F, Kopf M. Dual role of the IL-12/IFN-γ axis in the development of autoimmune myocarditis: Induction by IL-12 and protection by IFN-γ. J Immunol 2001;167:5464–9.
[32] Afanasyeva M, Wang Y, Kaya Z, Stafford EA, Dohmen KM, Sadighi Akha AA, et al. Interleukin-12 receptor/STAT4 signaling is required for the development of autoimmune myocarditis in mice by an interferon-γ independent pathway. Circulation 2001;104:3145–51.
[33] Song HK, Noorchashm H, Lin TH, Moore DJ, Greeley SA, Caton AJ, et al. Specialized CC-chemokine secretion by Th1 cells in destructive autoimmune myocarditis. J Autoimmun 2003;21. 295–230.
[34] Vidal SM, Malo D, Bogan K, Skamene E, Gros P. Natural resistance to infection with intracellular parasites: isolation of a candidate for BCG. Cell 1993;73:469–85.
[35] Brown DH, Lafuse W, Zwilling BS. Cytokine-mediated activation of macrophage form *Mycobacterium bovis* BCG-resistant and -susceptible mice: Differential effects corticosterone on antimycobacterial activity and expression of the Bcg gene (candidate Nramp). Infect Immun 1995; 63:2983–8.
[36] Mnaca C, Reed MB, Freeman S, Mathema B, Kreiswirth B, Barry III CE, et al. Differential monocyte activation underlies strain-specific *Mycobacterium tuberculosis* pathogenesis. Infect Immun 2004;72:5511–4.
[37] Fairweather DL, Frisancho-Kiss S, Rose NR. Viruses as adjuvants for autoimmunity: evidence from Coxsackievirus-induced myocarditis. Rev Med Virol 2004;15:17–27.
[38] Eriksson U, Ricci R, Hunziker L, Kurrer MO, Oudit GY, Watts TH, et al. Dendritic cell-induced autoimmune heart failure requires cooperation between adaptive and innate immunity. Nat Med 2003;9:1484–90.
[39] Bullet Y, Faure E, Thomas L, Equils O, Arditi M. Cooperation of Toll-like receptor 2 and 6 for cellular activation by soluble tuberculosis factor and *Borrelia burgdorferi* outer surface protein A lipoprotein: role of Toll-interacting protein and IL-1 receptor signaling molecules in Toll-like receptor 2 signaling. J Immunol 2001;167:987–94.
[40] Schner M, Barton GM, Holt AC, Takeda K, Akira S, Medzhitov R. Roll-like receptors control activation of adaptive immune responses. Nat Immunol 2001;10:947–50.
[41] Jang S, Uematsu S, Akira S, Salgame P. IL-6 and IL-10 induction form dendritic cells in response to *Mycobacterium tuberculosis* is predominantly dependent on TLR2-mediated recognition. J Immunol 2004;173: 3392–7.
[42] Abreu MT, Arditi M. Innate immunity and Toll-like receptors: clinical implications of basic science research. J Pediatr 2004;144:421–9.
[43] Medina E, North RJ. Resistance ranking of some common inbred mouse strains of *Mycobacterium tuberculosis* and relationship to major histocompatibility complex haplotype and Nramp genotype. Immunology 1998; 93:270–4.

Available online at www.sciencedirect.com
ScienceDirect
Biochemical and Biophysical Research Communications 362 (2007) 281–287
BBRC
www.elsevier.com/locate/ybbrc

Structural analysis of obscurin gene in hypertrophic cardiomyopathy

Takuro Arimura [a,1], Yuji Matsumoto [a,b,1], Osamu Okazaki [c], Takeharu Hayashi [a], Megumi Takahashi [a], Natsuko Inagaki [a], Kunihiko Hinohara [a], Naoto Ashizawa [b], Keisuke Yano [b], Akinori Kimura [a,*]

[a] *Department of Molecular Pathogenesis, Medical Research Institute and Laboratory of Genome Diversity, School of Biomedical Science, Tokyo Medical and Dental University, 2-3-10 Kandasurugadai, Chiyoda-ku, Tokyo 101-0062, Japan*
[b] *Department of Cardiovascular Medicine, Course of Medical and Dental Sciences, Graduate School of Biomedical Sciences, Nagasaki University, Nagasaki 852-8501, Japan*
[c] *Division of Nephrology and Cardiology, International Medical Center, Tokyo 162-8655, Japan*

Received 17 July 2007
Available online 13 August 2007

Abstract

Hypertrophic cardiomyopathy (HCM) is a cardiac disease characterized by left ventricular hypertrophy with diastolic dysfunction. Molecular genetic studies have revealed that HCM is caused by mutations in genes for sarcomere/Z-band components including titin/connectin and its associate proteins. However, disease-causing mutations can be found in about half of the patients, suggesting that other disease-causing genes remain to be identified. To explore a novel disease gene, we searched for obscurin gene (*OBSCN*) mutations in HCM patients, because obscurin interacts with titin/connectin. Two linked variants, Arg4344Gln and Ala4484Thr, were identified in a patient and functional analyses demonstrated that Arg4344Gln affected binding of obscurin to Z9–Z10 domains of titin/connectin, whereas Ala4484Thr did not. Myc-tagged obscurin showed that Arg4344Gln impaired obscurin localization to Z-band. These observations suggest that the obscurin abnormality may be involved in the pathogenesis of HCM.

Keywords: Hypertrophic cardiomyopathy; Titin/connectin; Obscurin; Mutation; Protein–protein interaction

Hypertrophic cardiomyopathy (HCM) is characterized by hypertrophy and diastolic dysfunction of cardiac ventricles [1]. Although the etiology of HCM has not been fully elucidated, recent molecular genetic analyses have revealed that HCM is caused by mutations in the genes encoding components of sarcomere and/or Z-band including titin/connectin [1,2].

Sarcomere is a contractile unit of striated muscle composed of highly organized lattice of proteins [3]. Titin/connectin is a sarcomere component spanning the half sarcomere with the amino- and carboxyl-terminal ends positioned in the Z- and M-bands, respectively [4,5]. Titin/connectin is a key component in the sarcomere assembly, force transmission and maintenance of resting tension, *i.e.* it acts as a molecular ruler of the sarcomere and tethers various proteins including α-actinin, T-cap/telethonin, obscurin, α-actin, and cardiac myosin-binding protein C [5,6]. It has been reported that abnormalities of cardiac myosin-binding protein-C, α-actin, and T-cap/telethonin cause hereditary HCM [7–9]. We have previously reported two HCM-associated titin/connectin gene (*TTN*) mutations, Arg740Leu and Ser3799Tyr, located in the Z-band domain and heart-specific N2B domain in the I-band, respectively [10,11]. The Arg740Leu mutation decreased the binding to α-actinin [10], while the Ser3799Tyr mutation altered the binding to αB-crystallin [12] and FHL2 [13]. These observations indicated that the abnormal interactions between titin/connectin and its associated proteins could be molecular etiologies of HCM.

* Corresponding author. Fax: +81 3 5280 8055.
E-mail address: akitis@mri.tmd.ac.jp (A. Kimura).
[1] These authors contributed equally to this study.

0006-291X/$ - see front matter © 2007 Elsevier Inc. All rights reserved.
doi:10.1016/j.bbrc.2007.07.183

Obscurin, encoded by *OBSCN*, is a titin/connectin associated protein composed of multiple domains including immunoglobulin-like (Ig), Ca^{2+}/calmodulin binding, Rho guanine nucleotide exchange factor (Rho-GEF)-interacting domains [14,15]. The Ig domains 48 and 49 of obscurin interact with titin/connectin at the Z-band domains (Z9 and Z10) and at the I-band domain (novex-3), Ca^{2+}/calmodulin-binding domain interacts with calmodulin [14]. From these structures, it was suggested that obscurin was involved in the Ca^{2+}/calmodulin and G-protein-coupled signal transductions via the Ca^{2+}/calmodulin-binding domain and Rho-GEF domain, respectively. Obscurin also plays an important role in sarcomere organization during myofibrillogenesis and in regular alignment of sarcoplasmic reticulum [16]. In addition, expression of *OBSCN* was associated with myofibrillogenesis during cardiac hypertrophy [17,18].

In this study, we searched HCM patients for *OBSCN* variations and performed functional analyses of the identified *OBSCN* variants. We report here that abnormal interaction of titin/connectin with obscurin might be involved in the pathogenesis of HCM.

Materials and methods

Study population. We studied 144 genetically unrelated Japanese patients with HCM. Among them, apparent family histories were observed in 96 patients. All patients manifested with typical HCM phenotype as described previously [9,19]. Control subjects were 288 unrelated healthy Japanese selected at random. After acquiring informed consent, blood samples were obtained from each subject. The protocol for research was approved by the Ethics Reviewing Committee of Medical Research Institute, Tokyo Medical and Dental University.

Mutational analysis of OBSCN in HCM. Genomic DNA extracted from peripheral blood leukocytes of each individual was subjected to PCR by using of primer pairs specific to the analyzed regions covering *OBSCN* exons 50–53 and 54–56 which correspond to Ig48/49 (titin/connectin binding) and Ig51/52 (calmodulin binding) domains, respectively. We also investigated *TTN* mutations in the Z9/10 and novex-3 (obscurin binding) domains. Sequences of primers and PCR conditions are available upon request. PCR products from each patient were subjected to PCR-SSCP analysis as described previously [20]. When an abnormal SSCP pattern was observed, the PCR product was sequenced on both strands to determine the nucleotide change.

Alignment of obscurin sequences from various species. Protein sequence of human obscurin predicted from nucleotide sequence (GenBank Accession No. NM_052843) was aligned with those of bovine (XP_595102), dog (XP_539325), rat (XP_40808), and zebrafish (XP_691505). The mRNA sequences of bovine, dog, rat, and zebrafish were derived from annotated genomic sequences (GenBank Accession Nos. NW001495308, NW876258, NW047334, and NW646023, respectively). Prediction from nucleotide sequences to proteins and the alignments were performed using DNASIS Software (Hitachi).

Molecular modeling. The program SWISS-MODEL (http://swiss-model.expasy.org/SWISS-MODEL.html) [21] was used to build protein structure models according to the comparative protein modeling methodology, and 3D structure models of *OBSCN*-Ig48/49-WT and -Arg4344Gln + Ala4484Thr were drawn with Pymol (Delano Scientific, http://www.pymol.sourceforge.net/).

Mammalian two-hybrid (M2H) assay to analyze binding of titin/connectin with obscurin. We obtained cDNA fragments of human *TTN* and *OBSCN* by RT-PCR from human adult heart cDNA. Wild-type (WT) cDNA fragments of titin/connectin Z9/10 (from bp5101 to bp5787 of X_90568 corresponding aa1657–aa1885) and novex-3 domains (from bp15191 to bp15784 of NM_133379 corresponding aa4990–aa5187) were obtained by PCR. WT and Arg4344Gln cDNA fragments of obscurin Ig48–49 domains (from bp13071 to bp13634 of AJ002535 corresponding aa4334–aa4521) were also amplified by PCR. Ala4484Thr and Arg4344Gln + Ala4484Thr cDNA fragments of obscurin Ig48/49 domains were generated by primer-mediated mutagenesis. Detailed primer information is available upon request. The cDNA fragments were cloned into pCRII (Invitrogen) and excised by digestion by SalI and NotI. The excised cDNA fragments were cloned into p-ACT vector containing pVP16 as a prey (for *TTN*) and the p-BIND vector containing pGAL4 as a bait (for *OBSCN*) (CheckMate Mammalian two-hybrid system, Promega). These constructs were sequenced to ensure that no errors were introduced during the construction. M2H assays were performed as described previously [12]. Cells co-transfected with a combination of p-ACT-*TTN* cDNA based plasmids and p-BIND vectors, or p-ACT vectors and p-BIND-*OBSCN* cDNA based plasmids expressed virtually no luciferase activity.

Co-immunoprecipitation (co-IP) assay. Co-IP assays were performed as described previously [22]. Samples were electrophoresed on SDS–PAGE gels and transferred to a nitrocellulose membrane. After a pre-incubation with 5% skimmed milk in PBS, the membrane was incubated with primary rabbit anti-GAL4 polyclonal Ab (Santa Cruz Biotechnology) or anti-VP16 monoclonal Ab, and with secondary rabbit anti-mouse (for monoclonal Ab) or goat anti-rabbit (for polyclonal Ab) IgG HRP-conjugated Ab (1:2000, Dako A/S). Signals were visualized by enhanced chemiluminescence (PerkinElmer Life Science) and their densities were quantified by using ImageJ Version 1.36.

Indirect immunofluorescence microscopy. The p-BIND-*OBSCN* cDNA based plasmids were cleaved by digestion with BamHI and NotI and the *OBSCN* cDNA fragments were re-cloned into a BamHI-*Psp*OMI-cleaved pCMV-Tag3C (Stratagene) to obtain myc-tagged *OBSCN* WT, Arg4344Gln, Ala4484Thr or Arg4344Gln + Ala4484Thr. Obtained clones were sequenced to ensure no errors were introduced.

Care and treatment of animals were in accordance with the guidelines of National Institute of Health (NIH Publication 85-23, revised 1985) and subjected to prior approval by the local animal protection authority. Neonatal cardiomyocytes were isolated from one day-old Sprague–Dawley rats and prepared as described previously [23,24]. Cells were plated and transfected as described previously [12]. Forty-eight hours after the transfection, cells were washed with PBS, fixed for 15 min in 100% ethanol at −20 °C, incubated in a blocking solution (3% bovine serum, 0.03% Triton-X in PBS), and reacted with primary mouse anti-α-actinin monoclonal Ab (1:800, Sigma–Aldrich) or anti-MLC2v monoclonal Ab (1:1000, Synaptic System), and rabbit anti-myc tag polyclonal Ab (1:100, Santa Cruz Biotechnology), followed by secondary Alexa fluor 568 goat anti-mouse IgG (1:500, Molecular Probes) and FITC-conjugated sheep anti-rabbit IgG (1:200, Chemicon). Images of over 200 cells mounted on cover-glass using Mowiol 4-88 Reagent (Calbiochem) were analyzed with an LSM510 laser-scanning microscope (Carl Zeiss).

Statistical analysis. Numerical data from M2H and co-IP assays were expressed arbitrarily as means ± standard deviation (SD). Statistical differences were examined by student's *t*-test and *p* values of less than 0.05 were considered to be statistically significance.

Results

Identification of OBSCN variations

Sequence variations of *OBSCN* in the titin/connectin binding (Ig48/49) and calmodulin binding (Ig51/52) domains were searched in the patients and 17 variations were identified. These variations other than Arg4344Gln (c.13031G>A in exon 51), Ala4484Thr (c.13450G>A in exon 52), and Arg4381Cys were found in the SNP database

and/or in the controls. The Arg4381Cys variant found in a patient was not co-segregated with the disease in the multiplex family, indicating that it was a rare polymorphism (Fig. 1A). In clear contrast, Arg4344Gln and Ala4484Thr were found in a 19 year-old male patient in heterozygous state (Fig. 1B). Cloning and sequencing the PCR product showed that these variations were linked in *cis* (data not shown). These variations were found neither in the 576 control chromosomes nor in his unaffected father, implying that the variant allele was inherited from his mother who was affected with HCM. However, we could not confirm the co-segregation, because blood samples from his mother was not obtained for genetic test. Alignment of obscurin sequences demonstrated that both Arg4344 and Ala4484 were evolutionary conserved (Fig. 1C).

Sequence variations of *TTN* in the obscurin-binding Z9, Z10, and novex-3 domains were investigated in the patients and Pro1698Leu was found in the Z10 domain. However, this *TTN* variation was also found in the controls, suggesting that it was a polymorphism not related with HCM (data not shown).

Modeling structure of obscurin Ig48/49

Structure of the obscurin Ig48/49 domains was predicted by comparative modeling using the crystal structure of human N2B-titin/connectin isoform (PDB id: 2F8V, 2A38, and 1YA5) as template. Fig. 2A shows two representative 3D structures (rotated about *y*-axis by 180°) of the WT (control) or Arg4344Gln + Ala4484Thr (mutant) obscurin Ig48/49 domains. In these 3D models, residues 4344 and 4484 were situated on the opposite side by *y*-axis (circles and squares in Fig. 1D, respectively). The surface structure was modified by the Arg4344Gln variation, whereas the Ala4484Thr caused no obvious change. The other variations in the Ig48/49 domains found in this study did not cause any remarkable structural changes in the model (data not shown).

Functional alterations caused by the obscuring variant Arg4344Gln

To investigate the functional alterations caused by the *OBSCN* variations, Arg4344Gln and Ala4484Thr, in binding to Z9/10 or novex-3 domains of tinin/connectin, we used the M2H assay. A bait plasmid containing the *OBSCN*-Ig48/49 domains from WT or variant (Arg4344Gln, Ala4484Thr, and both Arg4344Gln and Ala4484Thr) was co-transfected with a prey plasmid containing *TTN* Z9/10 or novex-3 domains and luciferase activities were measured. When the luciferase activity in transfectants containing *OBSCN*-Ig48/49-WT and *TTN*-Z9/10 constructs was expressed as 1.00 arbitrarily unit (AU), those of *OBSCN*-Ig48/49-Arg4344Gln or *OBSCN*-Ig48/49-Arg4344Gln + Ala4484Thr constructs in combination with *TTN*-Z9/10 construct were significantly low (0.95 ± 0.028 AU, $p < 0.05$ or 0.81 ± 0.159 AU, $p < 0.01$, respectively). In contrast, the luciferase activity in transfectants of *OBSCN*-Ig48/49-Ala4484Thr and *TTN*-Z9/10 constructs was virtually unchanged (1.01 ± 0.065 AU). We next investigated the luciferase activities of the transfectants of *OBSCN*-Ig48/49 and *TTN*-novex-3 constructs. The activity in the transfectants of *OBSCN*-Ig48/49-WT and *TTN*-novex-3 constructs was lower (0.35 ± 0.013 AU) than that of *OBSCN*-Ig48/49-WT and *TTN*-Z9/10, and those in the transfectants of *OBSCN*-Ig48/49-Arg4344Gln, *OBSCN*-Ig48/49-Ala4484Thr or *OBSCN*-Ig48/49-Arg4344Gln + Ala4484Thr in combination with *TTN*-novex-3 were similar (0.38 ± 0.031, 0.37 ± 0.008 or 0.39 ± 0.016 AU, respectively) to that of *OBSCN*-Ig48/49-WT and *TTN*-novex-3.

To demonstrate the functional change by another method, we investigated the interaction by using co-IP assay. Western blot analysis of immunoprecipitates from the transfectants of WT or variant *OBSCN*-Ig48/49 in combination with WT *TTN*-Z9/10 revealed that, despite equal expression of proteins, the *OBSCN*-Ig48/49 in the presence of Arg4344Gln or Arg4344Gln+Ala4484Thr bound to *TTN*-Z9/10 significantly less (0.38 ± 0.14 or 0.23 ± 0.13 AU, respectively) than WT *OBSCN*-Ig48/49, when the binding between WT *OBSCN*-Ig48/49 and *TTN*-Z9/10 was expressed as 1.00 (Fig. 2A, $p < 0.001$ for each case). In contrast, binding of *OBSCN*-Ig48/49-Ala4484Thr with *TTN*-Z9/10 was similar to that of WT *OBSCN*-Ig48/49 with *TTN*-Z9/10 (1.06 ± 0.15 AU) (Fig. 2A). Consistent with the results of M2H assay, the lower binding of WT *OBSCN*-Ig48/49 and *TTN*-novex-3 was demonstrated by using co-IP assay (0.16 ± 0.095 AU) (Fig. 2A). The interactions of *TTN*-novex-3 and *OBSCN*-Ig48/49 in the presence of mutations were not significantly different (0.10 ± 0.039, 0.19 ± 0.042 or 0.12 ± 0.075 AU, respectively) as compared with that of *TTN*-novex-3 and WT *OBSCN*-Ig48/49 (Fig. 2A).

Altered incorporation of Arg4344Gln obscurin into Z-band

Because Ig48–51 domains of obscurin localize at the band, we examined cellular localization of WT or variant *OBSCN*-Ig48/49. Rat cardiomyocytes were transfected with myc-tagged WT or variant *OBSCN* constructs, co-immunostained for myc and α-actinin (Z-band marker), and examined under confocal microscopy. We observed that WT and variant myc-OBSCN-Ig48/49 proteins expressed at similar level in the transfected cells, as assessed by Western blot analyses (data not shown), suggesting that the variations did not affect the expression level of obscurin constructs. Control cells expressing myc-tag alone showed negative staining for myc-tag with striated staining pattern of sarcomeric α-actinin at the Z-band (data not shown). While the WT myc-*OBSCN*-Ig48/49 and Ala4484Thr myc-*OBSCN*-Ig48/49 were mainly targeted to the Z-band (Fig. 2Ba and c, respectively), myc-*OBSCN*-Ig48/49 carrying either Arg4344Gln or Arg4344Gln + Ala4484Thr variations showed less signals at the Z-band in about 60% of

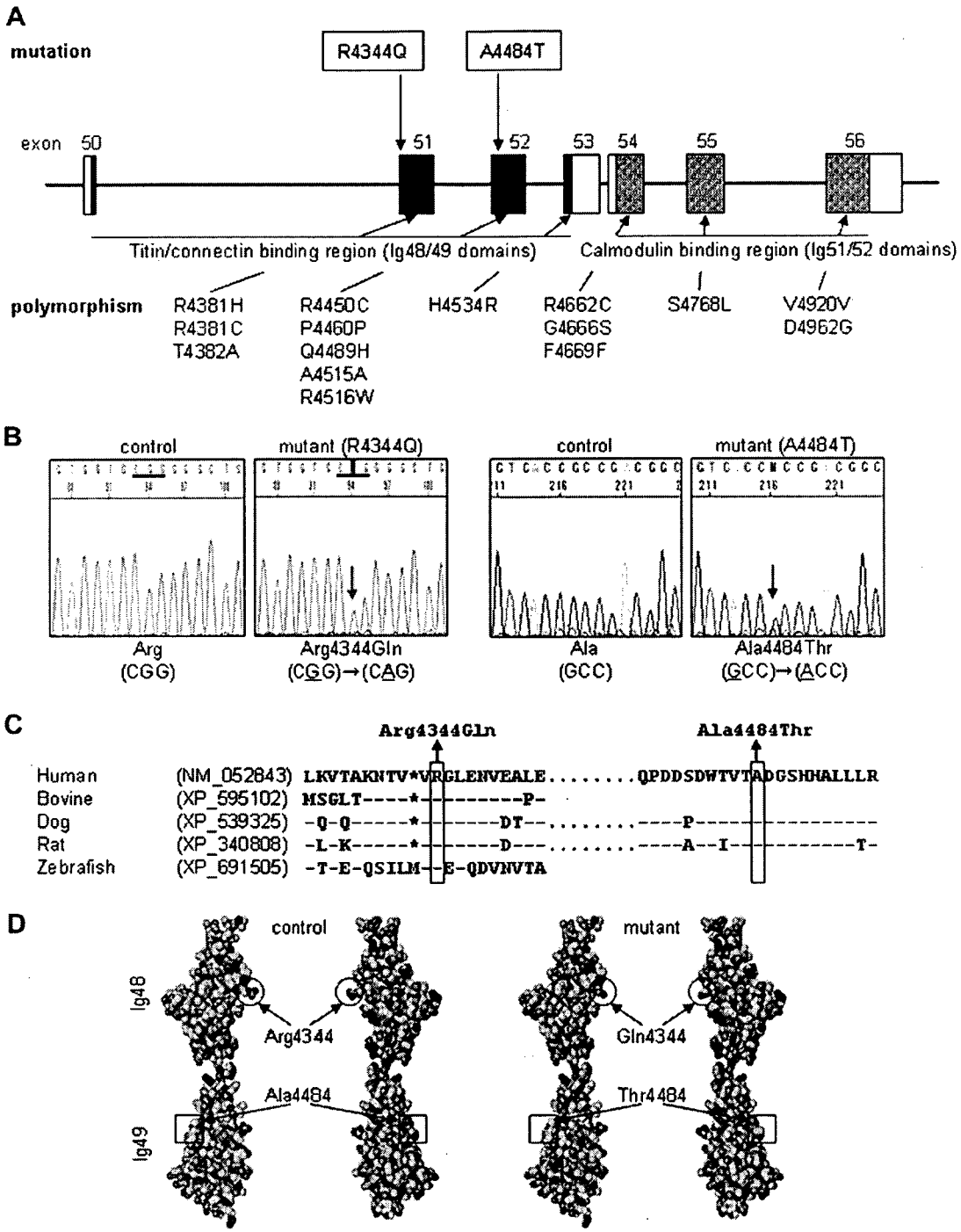

Fig. 1. Mutational analysis of *OBSCN* in HCM. (A) Sequence variations found in this study are listed. Single letter code was used to indicate the amino acid residue. *Solid boxes* represent titin/connectin-binding region of obscurin Ig48/49 domains corresponding to exons 50–53. *Dotted boxes* indicate calmodulin-binding region of obscurin Ig51/52 domains encoded by exons 54–56. (B) Direct sequencing data of *OBSCN* exons 51 and 52 from a control (left) and the HCM patient (right). Codons 4344 and 4484 of the control were CGG (Arg) and GCC (Ala), whereas the patient was heterozygous for CAG (Gln) and ACC (Thr), respectively. (C) Amino acid sequence alignment of obscurin from various species around the mutations. Protein sequence of human obscurin predicted from nucleotide sequence was aligned with that of bovine, dog, rat, and zebrafish. The mutation sites are boxed. Arg4344Gln and Ala4484Thr mutations found in this study are indicated. (D) 3D models of obscurin Ig48/49 domains in the presence of Arg4344Gln and Ala4484Thr. Different surface views (rotated about *y*-axis by 180°, upper or lower panels) of the obscurin Ig48/49 domains WT (left) and Arg4344Gln + Ala4484Thr (right). The mutation sites are indicated by circle (Arg4344Gln) and square (Ala4484Thr). Carbon, nitrogen and oxygen are shown as green, blue, and red spheres, respectively. (For interpretation of color mentioned in this figure legend the reader is referred to the web version of the article.)

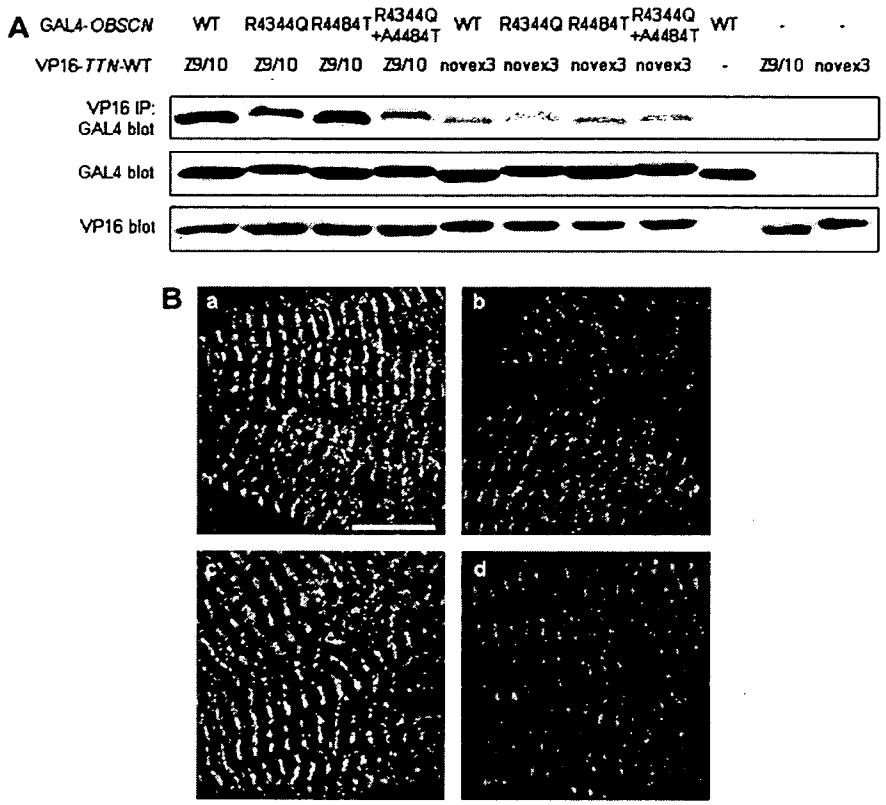

Fig. 2. Functional alterations caused by the OBSCN mutations. (A) Bindings of obscurin Ig48/49 domains with titin/connectin in co-immunoprecipitation pull-down (co-IP) analysis. Co-IP assay performed using an anti-VP16 antibody. Co-precipitated GAL4-obscurin was detected by immunoblot using an anti-GAL4 antibody (top panel). Expressions of GAL4-obscurin (middle panel) and VP16-titin/connectin Z9/10 or novex-3 domains (lower panel) were confirmed by immunoblot of whole cell supernatants. Dashes indicate only GAL4 or VP16 proteins (transfected only pBIND or pACT vectors, respectively). (B) Immunofluorescence staining and confocal microscopy of neonatal rat cardiomyocytes. Cultured day 4 neonatal rat cardiomyocytes transfected with myc-tagged WT, Arg4344Gln, Ala4484Thr or Arg4344Gln + Ala4484Thr obscurin Ig48/49 domains were stained with an anti-myc polyclonal antibody (FITC, green, to detect exogenous obscurin Ig48/49 domains). Typical examples showed correct Z-band incorporation of the Ig48/49 WT and Ala4484Thr obscurin (a and c, respectively), while impaired localization of Arg4344Gln and Arg4344Gln + Ala4484Thr obscurin Ig48/49 was observed (b and d, respectively). (For interpretation of color mentioned in this figure legend the reader is referred to the web version of the article.)

transfected cells (Fig. 2Bb and d, respectively). These data suggested less incorporation of Arg4344Gln obscurin into the Z-band, although the Z-band organization was not affected. The cells transfected with myc-tagged WT or mutant *OBSCN* constructs were co-immunostained for myc and MLC2v (A-band marker), and there was no obvious changes in MLC2v localization (data not shown).

Discussion

In the present study, we found two linked *OBSCN* variations, Arg4344Gln and Ala4448Thr, in a patient. They were not found in the control subjects and affected the evolutionary conserved residues of obscurin. Functional analyses showed that only the Arg4344Gln variant altered the functions of obscurin; *i.e.* conformation change in the surface structure of Ig48 domain in the 3D modeling, decreased binding to titin/connectin Z9/10 in both M2H and IP assays, and altered incorporation into the Z-band, suggesting that the Arg4344Gln might be involved in the pathogenesis of HCM in this patient.

Because obscurin Ig51/52 domains bind to calmodulin, the decreased binding of obscurin Ig48/49 domains to titin/connectin Z9/10 may lead to altered recruitment of calmodulin to the Z–I band and hence might affect the intracellular signaling. Obscurin has a similarity to Unc-89 that plays an important role in the assembly of myofibrils in *Caenorhabditis elegans* [25,26], and *Unc-89* mutation caused disorganization of muscle [27]. In addition, shut-off of obscurin expression in zebrafish lead to abnormalities in cardiac sarcomere alignment and function [28]. These studies suggested an important role of obscurin in structure and/or function of striated muscles.

In summary, we identified *OBSCN* Arg4344Gln mutation in HCM, which impaired the interaction of obscurin with titin/connectin. Although the molecular mechanisms of HCM due to the *OBSCN* mutation remain to be elucidated, our observations suggest that obscurin is indispensable to maintain the cardiac function in humans.

Acknowledgments

We are grateful Drs. H. Toshima, H. Nishi, Y. Koga, Matsumori, S. Sasayama, R. Nagai, and Y. Yazaki for their contributions in blood sampling from the patients. We also thank Dr. M. Yanokura, Ms. M. Emura and Ms. A. Nishimura for their technical assistances. This work was supported in part by Grants-in-Aid from the Ministry of Education, Culture, Sports, Science, and Technology, Japan, research grants from the Ministry of Health, Labor and Welfare, Japan, and the Program for Promotion of Fundamental Studies in Health Sciences of the National Institute of Biomedical Innovation (NIBIO), and research grants from Mitsubishi Pharma Research Foundation, Miyata Foundation for cardiac disease research, and "Association Française contre les Myopathies" (AFM, Grant No. 11737).

References

[1] P. Richardson, W. McKenna, M. Bristow, B. Maisch, B. Mautner, J. O'Connell, E. Olsen, G. Thiene, J. Goodwin, I. Gyarfas, I. Martin, P. Nordet, Report of the 1995 World Health Organization/International Society and Federation of Cardiology Task Force on the Definition and Classification of cardiomyopathies, Circulation 93 (1996) 841–842.

[2] B.J. Maron, J.A. Towbin, G. Thiene, C. Antzelevitch, D. Corrado, D. Arnett, A.J. Moss, C.E. Seidman, J.B. Young, Contemporary definitions and classification of the cardiomyopathies: an American Heart Association Scientific Statement from the Council on Clinical Cardiology, Heart Failure and Transplantation Committee; Quality of Care and Outcomes Research and Functional Genomics and Translational Biology Interdisciplinary Working Groups; and Council on Epidemiology and Prevention, Circulation 113 (2006) 1807–1816.

[3] D. Frank, C. Kuhn, H.A. Katus, N. Frey, The sarcomeric Z-disc: a nodal point in signalling and disease, J. Mol. Med 84 (2006) 446–468.

[4] L. Tskhovrebova, J. Trinick, Titin: properties and family relationships, Nat. Rev. Mol. Cell. Biol. 4 (2003) 679–689.

[5] H.L. Granzier, S. Labeit, The giant protein titin: a major player in myocardial mechanics, signaling, and disease, Circ. Res. 94 (2004) 284–295.

[6] E. Flashman, C. Redwood, J. Moolman-Smook, H. Watkins, Cardiac myosin binding protein C: its role in physiology and disease, Circ. Res. 94 (2004) 1279–1289.

[7] G. Bonne, L. Carrier, J. Bercovici, C. Cruaud, P. Richard, B. Hainque, M. Gautel, S. Labeit, M. James, J. Beckmann, J. Weissenbach, H.P. Vosberg, M. Fiszman, M. Komajda, K. Schwartz, Cardiac myosin binding protein-C gene splice acceptor site mutation is associated with familial hypertrophic cardiomyopathy, Nat. Genet. 11 (1995) 438–440.

[8] J. Mogensen, I.C. Klausen, A.K. Pedersen, H. Egeblad, P. Bross, T.A. Kruse, N. Gregersen, P.S. Hansen, U. Baandrup, A.D. Borglum, Alpha-cardiac actin is a novel disease gene in familial hypertrophic cardiomyopathy, J. Clin. Invest. 103 (1999) R39–R43.

[9] T. Hayashi, T. Arimura, M. Itoh-Satoh, K. Ueda, S. Hohda, N. Inagaki, M. Takahashi, H. Hori, M. Yasunami, H. Nishi, Y. Koga, H. Nakamura, M. Matsuzaki, B.Y. Choi, S.W. Bae, C.W. You, K.H. Han, J.E. Park, R. Knoll, M. Hoshijima, K.R. Chien, A. Kimura, Tcap gene mutations in hypertrophic cardiomyopathy and dilated cardiomyopathy, J. Am. Coll. Cardiol. 44 (2004) 2192–2201.

[10] M. Satoh, M. Takahashi, T. Sakamoto, M. Hiroe, F. Marumo, A. Kimura, Structural analysis of the titin gene in hypertrophic cardiomyopathy: identification of a novel disease gene, Biochem. Biophys. Res. Commun. 262 (1999) 411–417.

[11] M. Itoh-Satoh, T. Hayashi, H. Nishi, Y. Koga, T. Arimura, T. Koyanagi, M. Takahashi, S. Hohda, K. Ueda, T. Nouchi, M. Hiroe, F. Marumo, T. Imaizumi, M. Yasunami, A. Kimura, Titin mutations as the molecular basis for dilated cardiomyopathy, Biochem. Biophys. Res. Commun. 291 (2002) 385–393.

[12] N. Inagaki, T. Hayashi, T. Arimura, Y. Koga, M. Takahashi, H. Shibata, K. Teraoka, T. Chikamori, A. Yamashina, A. Kimura, Alpha B-crystallin mutation in dilated cardiomyopathy, Biochem. Biophys. Res. Commun. 342 (2006) 379–386.

[13] Y. Matsumoto, T. Hayashi, N. Inagaki, M. Takahashi, S. Hiroi, T. Nakamura, T. Arimura, K. Nakamura, N. Ashizawa, M. Yasunami, T. Ohe, K. Yano, A. Kimura, Functional analysis of titin/connectin N2-B mutations found in cardiomyopathy, J. Muscle Res. Cell Motil. 26 (2005) 367–374.

[14] P. Young, E. Ehler, M. Gautel, Obscurin, a giant sarcomeric Rho guanine nucleotide exchange factor protein involved in sarcomere assembly, J. Cell Biol. 154 (2001) 123–136.

[15] M.L. Bang, T. Centner, F. Fornoff, A.J. Geach, M. Gotthardt, M. McNabb, C.C. Witt, D. Labeit, C.C. Gregorio, H. Granzier, S. Labeit, The complete gene sequence of titin, expression of an unusual approximately 700-kDa titin isoform, and its interaction with obscurin identify a novel Z-line to I-band linking system, Circ. Res. 89 (2001) 1065–1072.

[16] A. Kontrogianni-Konstantopoulos, D.H. Catino, J.C. Strong, S. Sutter, A.B. Borisov, D.W. Pumplin, M.W. Russell, R.J. Bloch, Obscurin modulates the assembly and organization of sarcomeres and the sarcoplasmic reticulum, FASEB J. 20 (2006) 2102–2111.

[17] A.B. Borisov, M.O. Raeker, A. Kontrogianni-Konstantopoulos, K. Yang, D.M. Kurnit, R.J. Bloch, M.W. Russell, Rapid response of cardiac obscurin gene cluster to aortic stenosis: differential activation of Rho-GEF and MLCK and involvement in hypertrophic growth, Biochem. Biophys. Res. Commun. 310 (2003) 910–918.

[18] A.B. Borisov, S.B. Sutter, A. Kontrogianni-Konstantopoulos, R.J. Bloch, M.V. Westfall, M.W. Russell, Essential role of obscurin in cardiac myofibrillogenesis and hypertrophic response: evidence from small interfering RNA-mediated gene silencing, Histochem. Cell Biol. (2005) 1–12.

[19] T. Arimura, T. Hayashi, H. Terada, S.Y. Lee, Q. Zhou, M. Takahashi, K. Ueda, T. Nouchi, S. Hohda, M. Shibutani, M. Hirose, J. Chen, J.E. Park, M. Yasunami, H. Hayashi, A. Kimura, A Cypher/ZASP mutation associated with dilated cardiomyopathy alters the binding affinity to protein kinase C, J. Biol. Chem. 279 (2004) 6746–6752.

[20] A. Kimura, H. Harada, J.E. Park, H. Nishi, M. Satoh, M. Takahashi, S. Hiroi, T. Sasaoka, N. Ohbuchi, T. Nakamura, T. Koyanagi, T.H. Hwang, J.A. Choo, K.S. Chung, A. Hasegawa, R. Nagai, O. Okazaki, H. Nakamura, M. Matsuzaki, T. Sakamoto, H. Toshima, Y. Koga, T. Imaizumi, T. Sasazuki, Mutations in the cardiac troponin I gene associated with hypertrophic cardiomyopathy, Nat. Genet. 16 (1997) 379–382.

[21] T. Schwede, J. Kopp, N. Guex, M.C. Peitsch, SWISS-MODEL: an automated protein homology-modeling server, Nucleic Acids Res. 31 (2003) 3381–3385.

[22] T. Arimura, T. Hayashi, Y. Matsumoto, H. Shibata, S. Hiroi, T. Nakamura, N. Inagaki, K. Hinohara, M. Takahashi, S.I. Manatsu, T. Sasaoka, T. Izumi, G. Bonne, K. Schwartz, A. Kimura, Structural analysis of four and half LIM protein-2 in dilated cardiomyopathy, Biochem. Biophys. Res. Commun. (2007).

[23] H. Naito, I. Melnychenko, M. Didie, K. Schneiderbanger, P. Schubert, S. Rosenkranz, T. Eschenhagen, W.H. Zimmermann, Optimizing engineered heart tissue for therapeutic applications as surrogate heart muscle, Circulation 114 (2006) 172–178.

[24] O. Nakagawa, Y. Ogawa, H. Itoh, S. Suga, Y. Komatsu, I. Kishimoto, K. Nishino, T. Yoshimasa, K. Nakao, Rapid transcriptional activation and early mRNA turnover of brain natriuretic peptide in cardiocyte hypertrophy. Evidence for brain natriuretic peptide as an "emergency" cardiac hormone against ventricular overload, J. Clin. Invest. 96 (1995) 1280–1287.

[25] M.W. Russell, M.O. Raeker, K.A. Korytkowski, K.J. Sonneman, Identification, tissue expression and chromosomal localization of human Obscurin-MLCK, a member of the titin and Dbl families of myosin light chain kinases, Gene 282 (2002) 237–246.
[26] S.B. Sutter, M.O. Raeker, A.B. Borisov, M.W. Russell, Orthologous relationship of obscurin and Unc-89: phylogeny of a novel family of tandem myosin light chain kinases, Dev. Genes Evol. 214 (2004) 352–359.
[27] R.H. Waterston, J.N. Thomson, S. Brenner, Mutants with altered muscle structure of *Caenorhabditis elegans*, Dev. Biol. 77 (1980) 271–302.
[28] M.O. Raeker, F. Su, S.B. Geisler, A.B. Borisov, A. Kontrogianni-Konstantopoulos, S.E. Lyons, M.W. Russell, Obscurin is required for the lateral alignment of striated myofibrils in zebrafish, Dev. Dyn. 235 (2006) 2018–2029.

nature medicine

Sema3a maintains normal heart rhythm through sympathetic innervation patterning

Masaki Ieda[1,2], Hideaki Kanazawa[1,2], Kensuke Kimura[1], Fumiyuki Hattori[1], Yasuyo Ieda[1], Masahiko Taniguchi[3], Jong-Kook Lee[4], Keisuke Matsumura[1,2], Yuichi Tomita[1], Shunichiro Miyoshi[2], Kouji Shimoda[5], Shinji Makino[1], Motoaki Sano[1], Itsuo Kodama[4], Satoshi Ogawa[2] & Keiichi Fukuda[1]

Sympathetic innervation is critical for effective cardiac function. However, the developmental and regulatory mechanisms determining the density and patterning of cardiac sympathetic innervation remain unclear, as does the role of this innervation in arrhythmogenesis. Here we show that a neural chemorepellent, Sema3a, establishes cardiac sympathetic innervation patterning. Sema3a is abundantly expressed in the trabecular layer in early-stage embryos but is restricted to Purkinje fibers after birth, forming an epicardial-to-endocardial transmural sympathetic innervation patterning. *Sema3a*$^{-/-}$ mice lacked a cardiac sympathetic innervation gradient and exhibited stellate ganglia malformation, which led to marked sinus bradycardia due to sympathetic dysfunction. Cardiac-specific overexpression of *Sema3a* in transgenic mice (*SemaTG*) was associated with reduced sympathetic innervation and attenuation of the epicardial-to-endocardial innervation gradient. *SemaTG* mice demonstrated sudden death and susceptibility to ventricular tachycardia, due to catecholamine supersensitivity and prolongation of the action potential duration. We conclude that appropriate cardiac Sema3a expression is needed for sympathetic innervation patterning and is critical for heart rate control.

Cardiac tissues are extensively innervated by autonomic nerves. The cardiac sympathetic nerves extend from the sympathetic neurons in stellate ganglia, which reside bilateral to the vertebrae. Previous studies have established regional differences in the sympathetic innervation of the heart in larger mammals[1,2]. Sympathetic nerve fibers project from the base of the heart into the myocardium and are located predominantly in the subepicardium in the ventricle[3,4]. The central conduction system, including the sinoatrial node, the atrioventricular node and the His bundle, is abundantly innervated as compared with the working myocardium[1,4–6]. The sympathetic nervous system augments cardiac performance by increasing heart rate, conduction velocity, myocardial contraction, and relaxation. Accordingly, unbalanced neural activation or suppression might trigger lethal arrhythmia in diseased hearts[7–10]. These findings have demonstrated that sympathetic innervation patterning is critical for effective cardiac performance; however, little is known about the developmental and regulatory mechanisms underlying cardiac sympathetic innervation patterning. Moreover, the consequence of its disruption remains unknown.

We and others have reported that nerve growth factor (NGF), a member of the neurotrophin family, is required for sympathetic axon growth and innervation in the heart[11,12]. However, the neural chemorepellent that induces growth cone collapse and repels sympathetic axons in the heart has not been identified. Sema3a is a class 3 secreted semaphorin and a potent neural chemorepellent for sensory and sympathetic axons[13–15]. Targeted inactivation of *Sema3a* disrupts neural patterning and projections, indicating the importance of Sema3a signaling for directional guidance of nerve fibers[16,17]. It remains unknown, however, whether cardiomyocytes produce Sema3a, and, if so, whether this protein affects sympathetic neural patterning and cardiac performance. Here we demonstrate the expression pattern of Sema3a in developing hearts and its critical roles in cardiac sympathetic innervation patterning and arrhythmia, using various gene-modified mouse models.

RESULTS

Sympathetic nerve distribution in mouse heart

We first analyzed the distribution of cardiac sympathetic nerves in adult mouse hearts at postnatal day (P) 42 by immunostaining with an antibody to tyrosine hydroxylase, a marker of sympathetic nerves. Tyrosine hydroxylase–immunopositive (TH^+) nerves were most abundant in the sinoatrial node, the atrioventricular node and the His bundle, as indicated by acetyl cholinesterase (AChE) activity staining (refs. 18,19 and **Fig. 1a**). In contrast, TH^+ nerves in Purkinje

[1]Department of Regenerative Medicine and Advanced Cardiac Therapeutics, Keio University School of Medicine, 35 Shinanomachi, Shinjuku-ku, Tokyo 160-8582, Japan. [2]Cardiology Division, Department of Medicine, Keio University School of Medicine, 35 Shinanomachi, Shinjuku-ku, Tokyo 160-8582, Japan. [3]Department of Biochemistry, Cancer Research Institute, Sapporo Medical University School of Medicine, S-1, W-17, Chuo-ku, Sapporo 060-8556, Japan. [4]Department of Cardiovascular Research, Research Institute of Environmental Medicine, Nagoya University, Furo-cho, Chikusa-ku, Nagoya 464-8601, Japan. [5]Laboratory Animal Center, Keio University School of Medicine, 35 Shinanomachi, Shinjuku-ku, Tokyo 160-8582, Japan. Correspondence should be addressed to K.F. (kfukuda@sc.itc.keio.ac.jp).

Received 9 November 2006; accepted 27 February 2007; published online 8 April 2007; doi:10.1038/nm1570

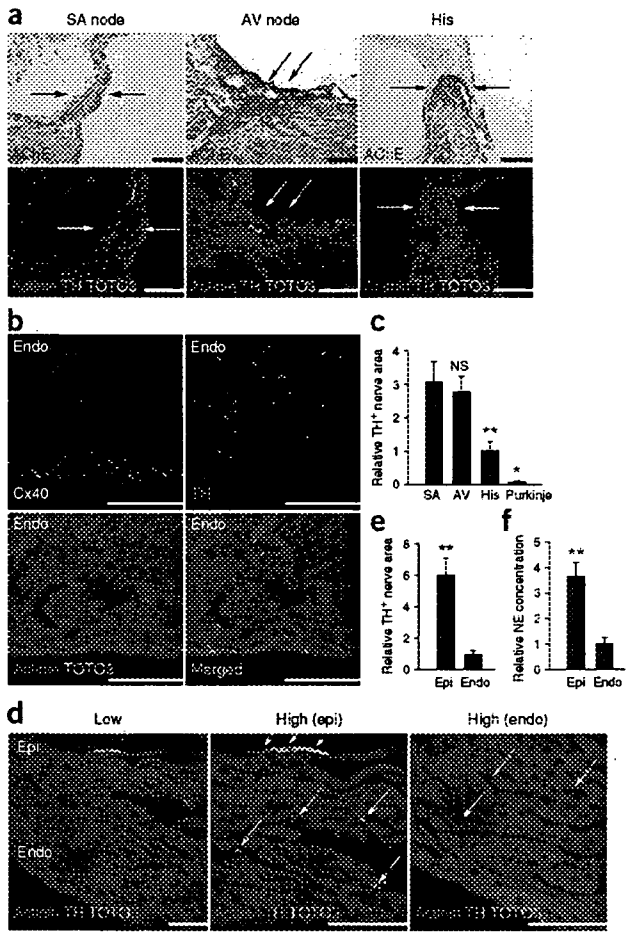

Figure 1 Regional heterogeneity of sympathetic innervation in the mouse heart. (**a**) The sinoatrial (SA) node, atrioventricular (AV) node and His bundle (arrows) stained with AChE (brown) were abundantly innervated by tyrosine hydroxylase–positive (TH^+) nerves. Top, acetyl cholinesterase (AChE) and hematoxylin staining. Bottom, immunofluorescent staining for α-actinin, tyrosine hydroxylase (TH) and TOTO3 (as a nuclear stain). (**b**) Immunofluorescent staining for α-actinin, TH, Cx40 and TOTO3 was performed. Few TH^+ nerves were detected in Purkinje fibers. (**c**) Quantitative analysis of TH^+ nerve areas ($n = 4$). (**d**) Immunofluorescent staining for α-actinin, TH and TOTO3. 'Low' and 'high' indicate low- and high-power fields, respectively. TH^+ nerves (arrows) were more abundant in the subepicardium (epi) than in the subendocardium (endo); quantitative data are shown in **e** ($n = 4$). (**f**) Cardiac norepinephrine (NE) concentration measured by high-performance liquid chromatography (HPLC) ($n = 6$). $^*P < 0.001$; $^{**}P < 0.01$; NS, not significant (in **c**, compared to SA). Scale bars, 100 μm.

fibers, which express connexin40 (Cx40)[20], were barely detectable and present in much smaller numbers than in the surrounding working myocardium (**Fig. 1b,c**). In the ventricular myocardium, TH^+ nerves were abundant and more so in the subepicardium than the subendocardium (**Fig. 1d,e**). The norepinephrine concentration was also significantly higher in the subepicardium (3.7-fold; **Fig. 1f**).

We next analyzed the time course of cardiac sympathetic innervation in developing mouse ventricles. Nerve endings appeared at embryonic day (E) 15 in the epicardial surface and were apparent in the myocardium at P7 and P42 (**Supplementary Fig. 1** online). Together, these results show that cardiac sympathetic nerve density exhibits regional differences, and that sympathetic nerve fibers in mice develop from the epicardial base of the heart into the myocardium, as observed in larger mammals[1,2,5].

Sema3a expression is inversely related to sympathetic innervation

To test whether Sema3a might be a signal for determining cardiac sympathetic innervation patterning, we analyzed heterozygous *Sema3a* knocked-in *lacZ* mice (*Sema3a*$^{lacZ/+}$) and determined *Sema3a* expression in the heart[16]. At E10, we observed *lacZ* expression in the forelimb buds and somites and weakly in the heart. *In situ* hybridization for *Sema3a* confirmed that *lacZ* expression in *Sema3a*$^{lacZ/+}$ mice correctly reflected endogenous gene expression (**Fig. 2a**). At E12, we detected strong *lacZ* expression in the heart, especially in the trabecular component of both ventricles (**Fig. 2b**). In E15 hearts, we observed *lacZ* expression at the subendocardium but not at the subepicardium in the atria and ventricles. At P1 and P42, *lacZ* expression was reduced in certain locations and highlighted the Purkinje fiber network along the ventricular free wall (**Fig. 2c**). To verify the presence of *lacZ*$^+$ cells in Purkinje fibers at P42, we immunostained sections with an antibody to Cx40 and found that ventricular subendocardial *lacZ*$^+$ cells also stained for Cx40 (**Fig. 2d**). In contrast, richly innervated and AChE-positive sinoatrial nodes (data not shown), atrioventricular nodes and His bundles did not express *lacZ* (**Fig. 2e**).

Quantitative RT-PCR of *Sema3a* in developing hearts also revealed that *Sema3a* mRNA was present from E12 and its levels then decreased in a linear fashion, in contrast to the sympathetic innervation (**Fig. 2f**). At P42, *Sema3a* mRNA expression was 2.3-fold higher in the subendocardium than in the subepicardium (**Fig. 2g**). These results indicated that *Sema3a* expression has an opposite time course and distribution from sympathetic innervation in developing hearts. Double staining with tyrosine hydroxylase and 5-bromo-4-chloro-3-indolyl-β-D-galactopyranoside (X-gal) revealed that most sympathetic nerves were restricted to the subepicardium at P1, when *Sema3a* was expressed extensively at the midcardial and subendocardial layers. At P42, sympathetic innervation extended vigorously into the ventricular myocardium, concomitant with *Sema3a* being downregulated and confined only to Purkinje fibers (**Fig. 2h**). Together, these results suggested that *Sema3a* is synthesized in Purkinje fibers and its expression is inversely related to the extent of sympathetic innervation.

Innervation patterning is disrupted in *Sema3a*$^{-/-}$ hearts

To investigate whether Sema3a is critical for cardiac sympathetic nerve development, we analyzed *Sema3a* homozygous null mice (*Sema3a*$^{-/-}$)[16]. Most *Sema3a*$^{-/-}$ mice die within the first postnatal week, and only 20% remain viable until weaning[16,17]. At P1, thick and fasciculated nerve fibers were restricted to the epicardial surface and few fibers were detected within the myocardium in the hearts of wild-type mice. In *Sema3a*$^{-/-}$ hearts, only a few fibers were observed at the epicardial surface, but many axons projected aberrantly into the myocardium at this early stage (**Fig. 3a,b**). To examine the overall pattern of cardiac sympathetic innervation, we performed whole-mount immunostaining for tyrosine hydroxylase at P1 on wild-type and *Sema3a*$^{-/-}$ hearts. Sympathetic nerve fibers appeared thinner and were fewer in number on the epicardial surface of *Sema3a*$^{-/-}$ hearts (**Fig. 3c**). At P14, when the sympathetic nerves extended into the myocardium, wild-type hearts showed a clear epicardial-to-endocardial gradient of sympathetic innervation. In contrast, sympathetic nerve density was reduced in the subepicardium but increased

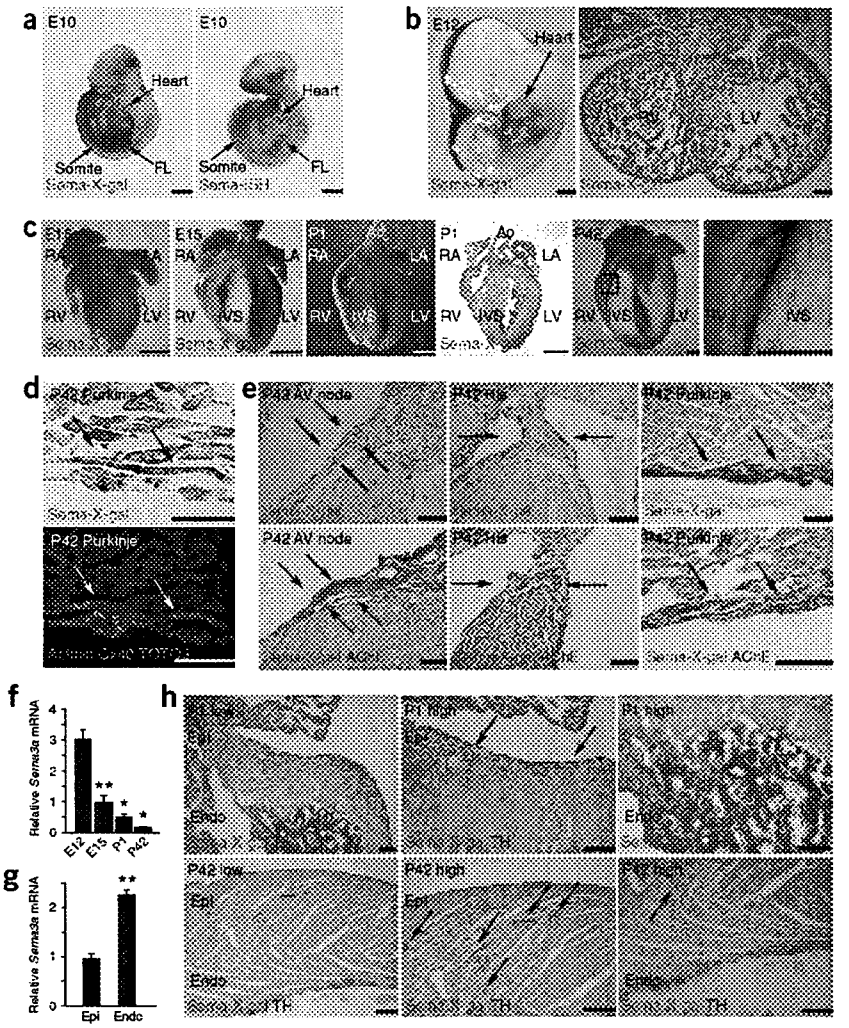

Figure 2 Inverse pattern of *Sema3a* expression and sympathetic innervation in developing hearts. (**a**) X-gal staining (green) of *Sema3a*$^{lacZ/+}$ at E10 (left). *In situ* hybridization (ISH) for *Sema3a* (right). (**b**) X-gal staining of *Sema3a*$^{lacZ/+}$ at E12 demonstrated strong *Sema3a* expression in the heart. (**c**) *lacZ* expression was observed in the subendocardium in *Sema3a*$^{lacZ/+}$ hearts at E15. The signal-positive areas were gradually reduced by P1 and P42, and a higher magnification view of the network of Purkinje fibers in P42 *Sema3a*$^{lacZ/+}$ hearts is shown in the far right micrograph. (**d**) X-gal staining (top) and triple immunofluorescence staining for α-actinin, Cx40 and TOT03 (bottom) in the subendocardium in P42 *Sema3a*$^{lacZ/+}$ hearts. Arrows indicate Purkinje fibers demarcated with Cx40. (**e**) X-gal staining (top), and double staining with AChE (brown) and X-gal (blue) (bottom) for the conduction system (arrows) in P42 *Sema3a*$^{lacZ/+}$ hearts. Note that AChE-positive AV node and His bundle did not express *lacZ*, but AChE-positive Purkinje fibers were colabeled with X-gal staining. (**f**) *Sema3a* mRNA expression in wild-type developing hearts determined by quantitative RT-PCR ($n = 5$). (**g**) *Sema3a* expression in the subendocardium and subepicardium in wild-type mice ($n = 5$). (**h**) Double staining with tyrosine hydroxylase (TH, brown) and X-gal (blue) in P1 and P42 *Sema3a*$^{lacZ/+}$ hearts. 'Low' and 'high' indicate low and high magnification, respectively. Note that sympathetic nerves were restricted to the subepicardium at P1, but extended into the myocardium at P42, coincident with downregulation of Sema3a. Representative data are shown in **a**–**e** and **h**. $^*P < 0.001$ and $^{**}P < 0.01$ (in **f**, compared to data at E12). FL, forelimb; RA, right atrium; LA, left atrium; RV, right ventricle; LV, left ventricle; IVS, interventricular septum; Ao, aorta. Scale bars: 50 μm in **d**; 100 μm in the right panel of **b**; 100 μm in **e**,**h**; 1 mm in all others.

in the subendocardium in *Sema3a*$^{-/-}$ mice, resulting in a marked reduction of the subepicardial-to-subendocardial ratio of sympathetic innervation (7.7-fold in wild-type and 0.8-fold in *Sema3a*$^{-/-}$ animals **Fig. 3d–f**).

Next, we performed double staining with X-gal and tyrosine hydroxylase in *Sema3a*$^{lacZ/+}$ (*Sema3a* heterozygous null) and *Sema3a*$^{lacZ/lacZ}$ (*Sema3a* homozygous null) hearts. *Sema3a*$^{lacZ/+}$ hearts showed a restricted sympathetic innervation within the working myocardium, and the axons never extended into the *Sema3a*-expressing Purkinje fibers. In *Sema3a*$^{lacZ/lacZ}$ hearts, we observed many aberrant projections at the subendocardium where *lacZ* was expressed, and sympathetic nerves grew freely over *lacZ*-expressing areas (**Fig. 3g**). These results indicated that Sema3a is critical for the patterning of cardiac sympathetic innervation.

Sema3a$^{-/-}$ mice exhibit sinus bradycardia

We next examined the central conduction system in *Sema3a*$^{-/-}$ hearts. The sinoatrial nodes, atrioventricular nodes and His bundles, demarcated with AChE activity staining, were intact in appearance in *Sema3a*$^{-/-}$ hearts. The sympathetic nerve density in the conduction system was also not different between wild-type and *Sema3a*$^{-/-}$ hearts (**Fig. 4a** and **Supplementary Fig. 2** online). To determine whether sympathetic neurons that project nerve fibers to the heart were disrupted, we examined the stellate ganglia. TH$^+$ neurons accumulated to form sympathetic ganglia at positions bilateral to the vertebrae in wild type mice. In contrast, the sympathetic neurons did not accumulate in *Sema3a*$^{-/-}$ mice but instead were distributed widely in a dislocated pattern (**Fig. 4b**). The stellate ganglia malformation was sustained at P42 in *Sema3a*$^{-/-}$ mice (data not shown).

To identify the effects of abnormal sympathetic neural distribution in the absence of Sema3a expression, we performed telemetric electrocardiography (ECG) in awake and free-moving wild-type and *Sema3a*$^{-/-}$ mice ($n = 5$ in both groups), of age 6 to 8 weeks. *Sema3a*$^{-/-}$ mice showed sinus bradycardia and abrupt sinus slowing, with a heart rate of 531 ± 27 beats per min compared with 604 ± 36 beats per min in wild-type mice (**Fig. 4c** and **Supplementary Table 1** online). To determine whether the bradycardia arose from intrinsic or extrinsic defects in the sinus node, we measured heart rate responses following pharmacological intervention. Blocking the sympathetic system with propranolol reduced the heart rate to a larger extent in the wild-type mice than in *Sema3a*$^{-/-}$ mice, suggesting that basal sympathetic activity was downregulated in *Sema3a*$^{-/-}$ hearts. In contrast, blocking parasympathetic activity had no substantial effect in either group of mice, consistent with previous reports showing that mice have weak